Weiwei Bian, Suo Wang, Yong Yao, Xianwei Jiao, Wenxiao Peng, Tianshui Yang, Shihong Zhang, Huaichun Wu, Haiyan Li, and Chenglong Deng, 2022, Location and shape of the Lhasa terrane prior to India-Asia collision: GSA Bulletin, https://doi.org/10.1130/B36647.1.

Supplemental Material

Figure S1. Hysteresis loops after high-field slope correction for the representative samples.

Figure S2. Temperature dependence of magnetic susceptibility (*k*-*T* curves) for representative samples.

Figure S3. Equal-area projections of the specimen-mean directions of the low-temperature component (LTC).

Figure S4. Equal-area projections of the site-mean directions of the middle-temperature component (MTC).

Table S1. Hysteresis parameter for individual specimens at room temperature.

Table S2. Middle-temperature component (MTC) directions for the Duoni formation red beds.

Table S3. High-temperature component (HTC) directions for the Duoni formation red beds.

Table S4. Summary of the available Cretaceous Paleomagnetic results from the Shiquanhe, Gerze, Cuoqin, Maxiang, Linzhou, and Naqu areas in the lhasa terrane.

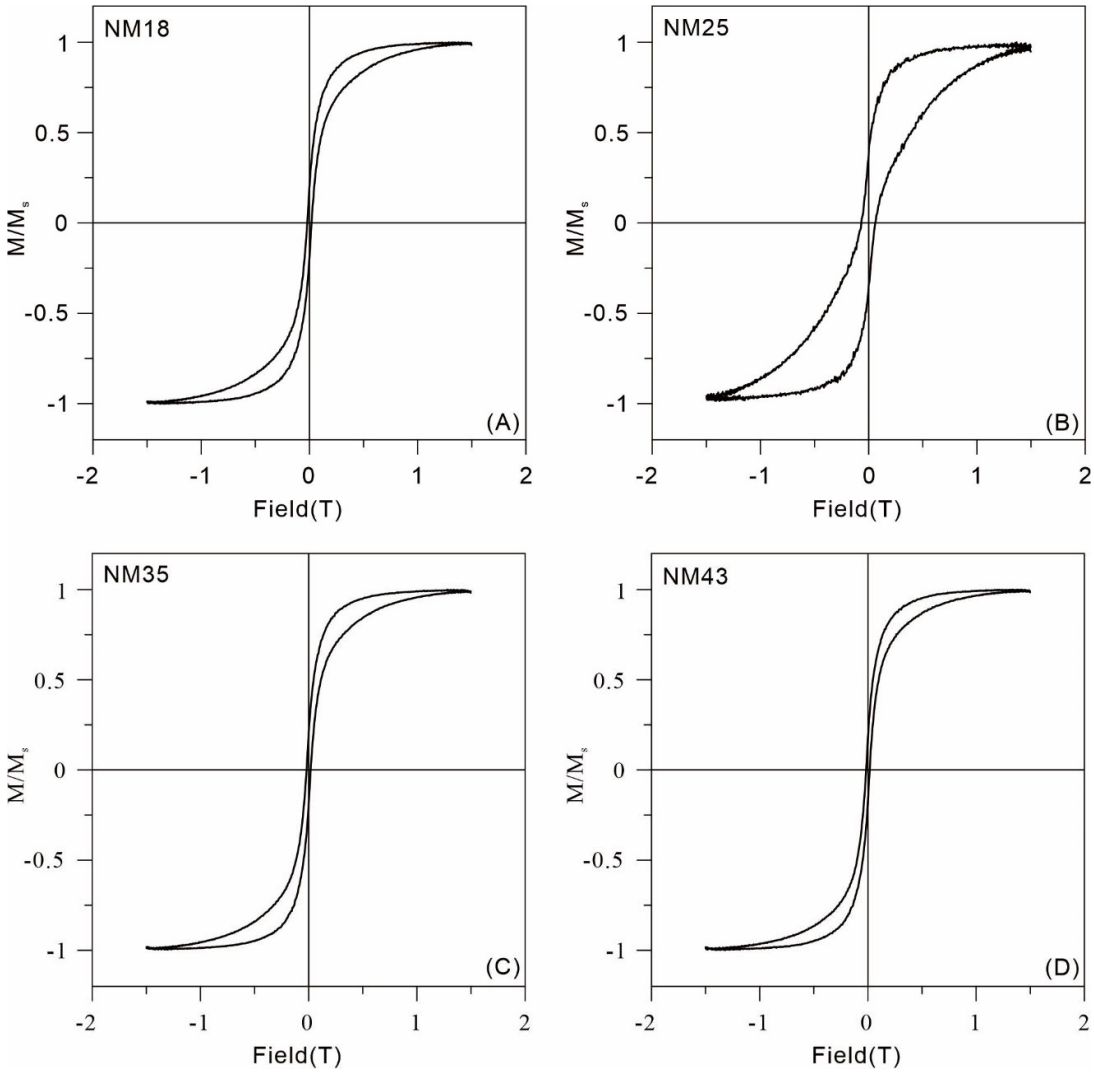

Figure S1. Hysteresis loops after high-field slope correction for the representative samples.

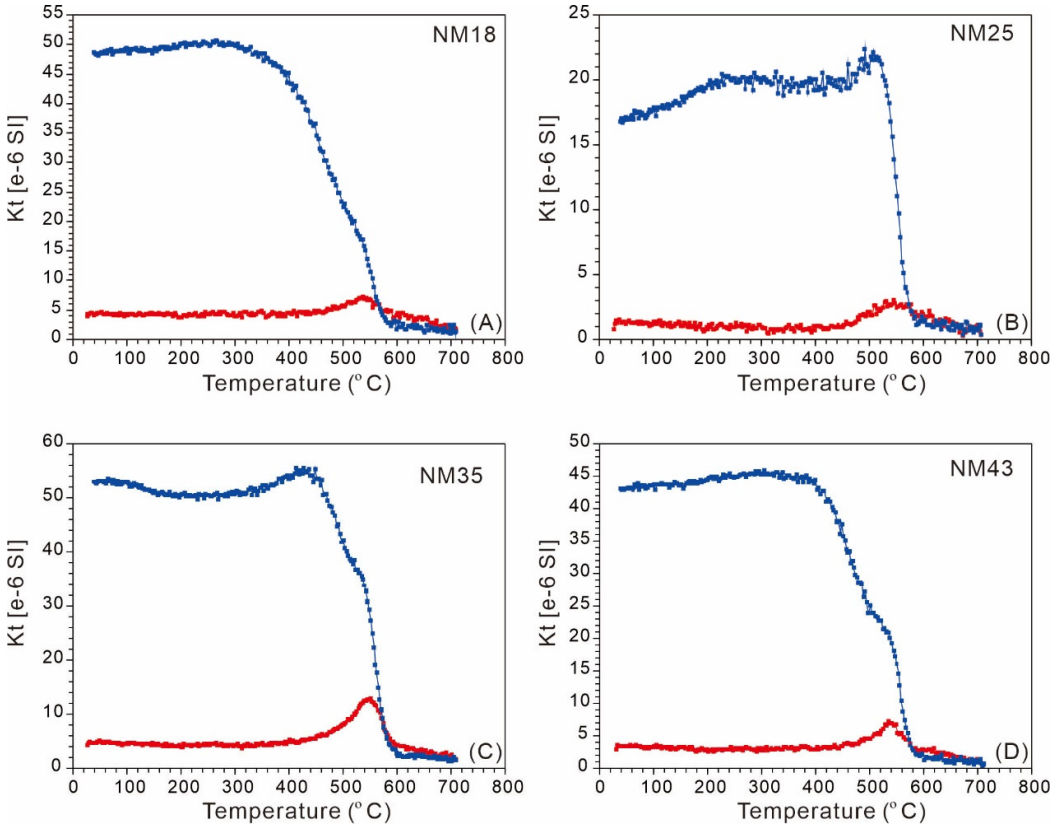

Figure S2. Temperature dependence of magnetic susceptibility (*k*-*T* curves) for representative samples.

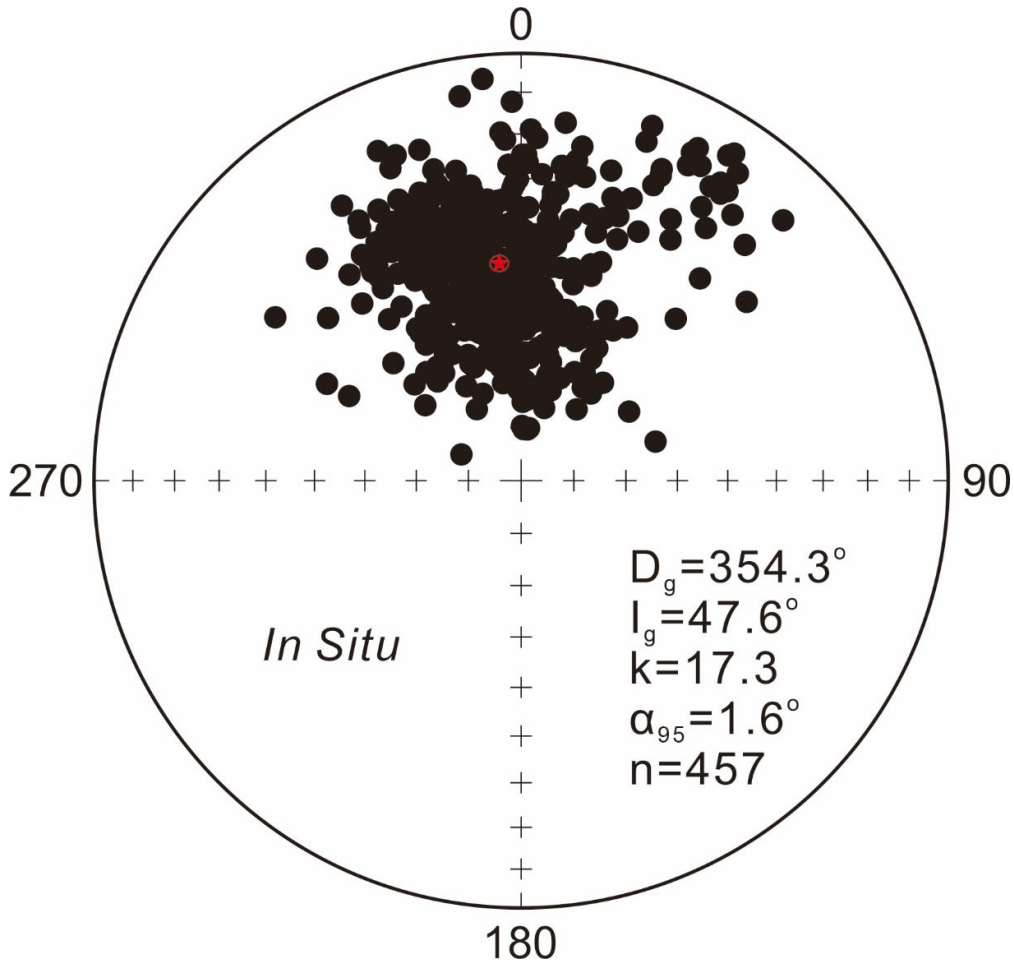

Figure S3. Equal-area projections of the specimen-mean directions of the low-temperature component (LTC).

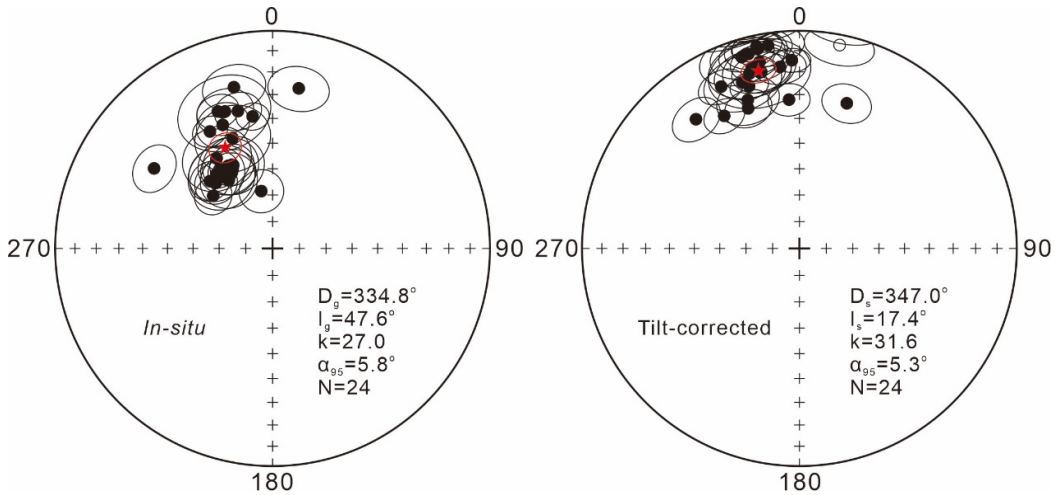

Figure S4. Equal-area projections of the site-mean directions of the middle-temperature component (MTC).

TABLE S1. HYSTERESIS PARAMETER FOR INDIVIDUAL SPECIMENS AT ROOM TEMPERATURE.

Sample	M_s Am^2/kg	M_{rs} Am^2/kg	B_c mT	B_{cr} mT	M_{rs}/M_s	B_{cr}/B_c
NM3	3.92E-06	9.28E-07	25.37	121.93	0.24	4.81
NM6	9.99E-06	1.46E-06	13.60	29.34	0.15	2.16
NM8	6.82E-06	9.97E-07	14.26	32.35	0.15	2.27
NM10	5.64E-06	1.00E-06	16.01	36.18	0.18	2.26
NM14	6.48E-06	9.69E-07	14.44	32.69	0.15	2.26
NM18	5.21E-06	1.03E-06	19.49	54.41	0.20	2.79
NM22	7.21E-06	1.16E-06	14.35	31.83	0.16	2.22
NM25	1.50E-06	5.60E-07	64.31	355.90	0.37	5.53
NM27	6.28E-06	1.16E-06	18.09	43.49	0.18	2.40
NM32	5.09E-06	1.01E-06	18.01	51.03	0.20	2.83
NM35	6.68E-06	1.33E-06	19.07	61.88	0.20	3.25
NM38	5.01E-06	9.07E-07	16.26	41.19	0.18	2.53
NM40	2.90E-06	6.82E-07	22.05	85.10	0.23	3.86
NM43	5.97E-06	1.05E-06	16.48	43.54	0.18	2.64
NM47	6.19E-06	1.12E-06	17.00	44.43	0.18	2.61
NM50	5.48E-06	9.20E-07	15.08	35.09	0.17	2.33

Note: B_c—coercive force; B_{cr}—remanent coercivity; M_{rs}—remanent saturation; M_s—saturation magnetization.

TABLE S2. MIDDLE-TEMPERATURE COMPONENT (MTC) DIRECTIONS FOR THE DUONI FORMATION RED BEDS.

Site	Strike/Dip (°)	N	In situ		Tilt-corrected		k	α_{95} (°)
			D_g (°)	I_g (°)	D_s (°)	I_s (°)		
NM1	295/21	5	340.3	33.8	347.1	17.9	24.8	15.7
NM2	302/24	8	345.8	35.2	353.9	17.2	49.9	7.9
NM4	297/33	9	9.3	26.4	11.2	-5.3	28.6	9.8
NM6	295/31	7	304.0	34.6	321.3	24.9	53.1	8.4
NM9	292/27	7	351.4	38.6	357.7	14.5	116.4	5.6
NM10	296/24	5	331.8	38.9	342.8	22.9	159.0	6.1
NM14	294/31	5	338.0	38.7	347.8	18.2	71.7	9.1
NM28	299/38	6	338.2	32.7	348.0	5.7	91.0	7.1
NM29	301/25	5	346.5	24.8	351.2	6.2	58.1	10.1
NM30	291/33	5	340.8	33.8	348.3	6.9	64.9	9.6
NM32	272/41	8	324.2	56.8	341.0	20.4	21.1	12.3
NM33	278/47	5	328.1	49.7	343.2	9.0	38.3	12.5
NM35	276/48	7	327.2	59.5	346.6	16.4	34.2	10.5
NM36	276/48	6	331.9	57.3	347.9	13.4	59.8	8.7
NM37	279/32	7	319.1	57.3	339.9	32.0	60.0	7.9
NM38	279/32	6	323.1	54.7	340.8	28.6	43.6	10.3
NM40	272/40	6	331.7	54.5	344.1	17.5	37.8	11.0
NM41	269/31	5	340.0	45.1	345.2	15.2	34.1	13.3
NM43	269/49	6	334.7	55.2	345.3	8.4	36.9	11.2
NM44	269/49	8	334.0	54.8	344.7	8.2	48.8	8.0
NM46	263/34	6	311.5	60.1	330.4	30.6	92.6	7.0
NM47	267/42	5	317.0	55.2	334.2	18.5	108.4	7.4
NM49	307/43	6	348.9	68.1	18.1	30.5	68.3	8.2
NM50	307/37	5	326.0	54.0	356.0	32.0	125.4	6.9
Overall mean A_0			334.8	47.6			27.0	5.8
N = 24 sites					347.0	17.4	31.6	5.3

Note: N—number of samples were used to calculate mean; $D_g/I_g(D_s/I_s)$—declination and inclination in geographic (stratigraphic) coordinates; k (K)—the best estimate of the precision parameter; α_{95}—the radius that the mean direction lies within 95% confidence. (1) Overall mean A_0 (N = 24 sites): ① The McElhinny (1964) fold test is inconclusive at 95% and 99% confidence levels: ks/kg = 1.17 < F(2*(n2-1), 2*(n1-1)) at 5% and 1% point = 1.63 and 2.00, respectively; ② The McFadden (1990) fold test is inconclusive at 95% and 99% confidence levels. "Xi" test: critical Xi at 95% = 5.70 and 99% = 8.01, respectively. "Xi1" and "Xi2" IS = 3.12 and 2.87, "Xi1" and "Xi2" TC = 12.03 and 10.66, respectively.

TABLE S3. HIGH-TEMPERATURE COMPONENT (HTC) DIRECTIONS FOR THE DUONI FORMATION RED BEDS.

Sample	Strike/Dip (°)	N	In situ		Tilt-corrected		MAD (°)
			D_g (°)	I_g (°)	D_s (°)	I_s (°)	
Site NM1 (31°35′8.4″N, 91°22′9.4″E)							
NM1-1A	295/21	5	318.8	31.8	328.2	21.7	3.1
NM1-2A	295/21	4	313.4	33.6	324.3	24.9	2.5
NM1-3A	295/21	5	315.3	18.4	320.2	10.2	3.1
NM1-4A	295/21	4	323.9	40.3	335.8	28.2	6.3
NM1-5A	295/21	8	318.8	31.9	328.2	21.7	2.1
NM1-6A	295/21	7	315.1	38.6	327.9	29.0	2.9
NM1-7A	295/21	5	321.6	37.3	332.7	25.9	4.0
NM1-8A	295/21	6	323.6	42.6	336.5	30.4	1.7
NM1-9A	295/21	4	310.6	32.9	321.6	25.2	2.3
Site NM2 (31°35′8.4″N, 91°22′9.7″E)							
NM2-1A	302/24	6	321.7	44.0	338.6	32.4	3.2
NM2-2A	302/24	6	330.0	39.3	342.8	25.5	4.3
NM2-3A	302/24	6	326.8	41.2	341.1	28.3	1.1
NM2-4A	302/24	7	319.0	38.2	333.6	28.2	4.0
NM2-5A	302/24	4	323.0	45.3	340.3	33.1	2.6
NM2-7A	302/24	5	321.0	43.4	337.8	32.1	3.4
NM2-8A	302/24	5	312.8	45.1	332.5	36.4	3.0
NM2-9A	302/24	6	318.9	39.2	334.0	29.0	1.1
NM2-10A	302/24	5	317.3	44.6	335.7	34.4	2.4
Site NM3 (31°35′8.4″N, 91°22′9.7″E)							
NM3-1A	303/26	7	319.1	43.6	337.8	32.1	4.5
NM3-2A	303/26	7	319.6	33.1	332.5	22.7	5.1
NM3-3A	303/26	6	324.2	25.6	332.8	14.2	4.1
NM3-4A	303/26	6	320.6	29.2	331.4	18.9	1.9
NM3-5A	303/26	7	324.4	42.0	340.8	28.8	2.3
NM3-7A	303/26	6	324.9	31.0	335.8	18.8	3.2
NM3-8A	303/26	7	321.8	25.6	330.9	15.2	3.5
NM3-9A	303/26	6	323.3	37.9	337.9	25.6	3.6
NM3-10A	303/26	7	323.5	31.9	335.1	20.2	5.8
Site NM4 (31°35′8.5″N, 91°22′9.6″E)							
NM4-1A	297/33	7	319.5	30.9	332.0	14.6	3.5
NM4-2A	297/33	6	317.6	26.1	328.0	11.4	3.1
NM4-3A	297/33	7	326.4	34.3	339.0	14.5	2.2
NM4-4A	297/33	7	324.1	28.8	334.5	10.8	3.6
NM4-6A	297/33	7	312.2	33.0	327.7	19.7	2.3

NM4-7A	297/33	7	329.4	43.5	345.8	21.4	2.4
NM4-8A	297/33	5	335.8	31.6	344.8	8.6	3.4
NM4-9A	297/33	6	327.0	28.7	336.6	9.4	2.7
NM4-10A	297/33	7	335.3	43.0	349.6	19.0	3.7
Site NM5 (31°35′8.5″N, 91°22′9.6″E)							
NM5-1A	290/43	7	325.5	46.0	344.2	14.5	3.9
NM5-2A	290/43	5	312.0	20.8	319.9	1.2	4.9
NM5-3A	290/43	6	336.6	47.9	351.9	12.1	6.4
NM5-4A	290/43	7	334.2	44.9	348.9	10.3	3.5
NM5-5A	290/43	5	322.9	41.8	340.2	12.2	3.1
NM5-7A	290/43	7	310.7	37.3	329.7	14.5	2.5
NM5-8A	290/43	4	326.6	45.5	344.6	13.7	9.0
NM5-10A	290/43	6	328.3	47.1	346.5	14.4	2.6
Site NM6 (31°35′8.5″N, 91°22′9.6″E)							
NM6-1A	295/31	6	337.7	31.2	345.5	8.3	6.0
NM6-2A	295/31	6	346.4	40.5	355.6	14.5	2.8
NM6-3A	295/31	5	302.2	38.4	322.4	28.8	4.7
NM6-4A	295/31	8	301.1	44.1	325.7	33.9	7.2
NM6-5A	295/31	6	325.5	29.3	335.0	11.0	3.7
NM6-6A	295/31	7	329.0	44.4	344.9	23.2	3.5
NM6-7A	295/31	6	304.1	50.3	332.5	37.4	5.0
NM6-9A	295/31	7	332.8	58.2	354.8	34.2	6.7
NM6-10A	295/31	6	315.3	22.6	323.6	9.4	9.3
Site NM7 (31°35′8.8″N, 91°22′9.6″E)							
NM7-1A	295/28	6	333.3	34.9	343.1	15.4	3.6
NM7-2A	295/28	6	320.8	30.9	331.4	16.1	1.9
NM7-5A	295/28	6	316.2	34.4	329.5	21.0	2.0
NM7-6A	295/28	6	319.7	34.3	332.2	19.6	2.3
NM7-7A	295/28	5	322.1	33.9	333.9	18.3	1.7
NM7-8A	295/28	7	7.1	40.4	11.1	13.4	1.7
NM7-9A	295/28	6	351.4	35.9	357.8	11.6	3.4
NM7-10A	295/28	6	323.7	30.4	333.5	14.6	6.9
NM7-11A	295/28	6	320.7	35.6	333.6	20.4	3.6
NM7-12A	295/28	6	321.1	37.1	334.6	21.5	4.3
Site NM8 (31°35′9.3″N, 91°22′9.7″E)							
NM8-1A	283/22	5	339.0	43.3	346.5	24.2	4.8
NM8-2A	283/22	4	340.5	42.3	347.4	23.0	7.6
NM8-3A	283/22	4	340.3	60.1	352.3	40.3	7.0
NM8-4A	283/22	5	301.9	42.9	317.4	32.9	6.7
NM8-6A	283/22	5	329.1	46.4	339.8	29.0	3.3
NM8-7A	283/22	7	332.0	43.5	341.2	25.7	2.6

NM8-8A	283/22	5	349.0	46.4	354.9	25.8	1.9
NM8-9A	283/22	6	318.1	52.7	334.4	37.3	6.6
NM8-10A	283/22	6	334.2	39.1	341.6	21.0	3.4
NM8-11A	283/22	7	307.6	41.7	321.4	30.0	3.8
Site NM9 (31°35′9.4″N, 91°22′9.8″E)							
NM9-1A	292/27	6	316.2	44.8	333.8	29.8	2.9
NM9-2A	292/27	5	308.3	45.6	328.6	33.2	3.7
NM9-3A	292/27	6	315.3	47.6	334.8	32.4	5.4
NM9-4A	292/27	6	317.2	35.5	329.8	21.1	3.3
NM9-5A	292/27	6	313.6	41.1	329.9	27.3	4.0
NM9-7A	292/27	5	316.0	46.1	334.4	30.9	2.3
NM9-8A	292/27	7	306.0	40.8	324.1	30.0	2.4
NM9-9A	292/27	6	308.0	39.6	324.9	28.2	2.7
NM9-10A	292/27	5	320.6	52.0	341.0	34.7	3.0
Site NM10 (31°35′9.9″N, 91°22′9.6″E)							
NM10-1A	296/24	5	327.5	39.1	339.4	24.3	5.2
NM10-2A	296/24	7	333.8	25.4	339.6	9.6	3.8
NM10-3A	296/24	4	340.5	25.2	345.4	7.5	8.5
NM10-4A	296/24	5	321.0	27.2	329.3	15.3	4.3
NM10-5A	296/24	5	323.0	33.6	333.6	20.6	3.3
NM10-7A	296/24	6	320.3	42.2	335.2	29.3	5.8
NM10-8A	296/24	6	321.7	43.8	337.1	30.3	3.5
NM10-10A	296/24	8	334.6	37.8	344.6	21.1	3.7
Site NM11 (31°35′10.3″N, 91°22′9.5″E)							
NM11-1A	297/29	6	326.1	42.7	339.9	28.0	1.7
NM11-2A	297/29	6	323.7	46.6	340.0	32.3	3.2
NM11-3A	297/29	4	332.8	46.7	346.7	29.8	3.1
NM11-4A	297/29	6	327.1	44.4	341.5	29.3	4.2
NM11-6A	297/29	5	325.0	34.2	335.4	20.5	1.2
NM11-7A	297/29	4	322.3	46.2	338.7	32.3	3.2
NM11-8A	297/29	6	328.4	42.6	341.6	27.3	3.0
NM11-11A	297/29	5	322.6	41.5	336.7	27.9	5.2
Site NM12 (31°35′12.3″N, 91°22′10.2″E)							
NM12-1A	299/29	4	319.5	49.4	341.2	32.9	5.7
NM12-2A	299/29	6	296.5	44.3	322.0	37.8	3.7
NM12-3A	299/29	4	321.5	46.9	341.0	30.0	1.9
NM12-4A	299/29	7	333.8	45.4	348.7	24.7	2.4
NM12-5A	299/29	5	310.6	44.5	332.1	32.1	5.8
NM12-6A	299/29	5	318.5	53.8	343.6	36.9	4.8
NM12-7A	299/29	7	316.5	47.6	338.1	32.5	1.8

NM12-8A	299/29	6	313.0	47.2	335.5	33.4	4.1
NM12-9A	299/29	6	328.9	50.0	347.8	30.4	2.7
Site NM13 (31°35′12.5″N, 91°22′10.2″E)							
NM13-1A	294/27	5	322.8	53.8	347.0	36.2	5.1
NM13-2A	294/27	8	318.7	40.3	335.9	26.2	5.3
NM13-3A	294/27	6	319.5	53.0	344.4	36.6	3.9
NM13-4A	294/27	5	307.8	28.5	320.9	20.6	6.4
NM13-5A	294/27	5	338.6	46.1	353.1	24.6	7.9
NM13-6A	294/27	6	338.9	32.8	347.7	12.2	5.4
NM13-7A	294/27	5	326.0	38.1	340.1	21.5	3.6
NM13-8A	294/27	4	317.4	63.0	351.2	45.2	5.4
NM13-9A	294/27	4	335.4	35.0	345.8	15.4	4.3
NM13-10A	294/27	5	325.2	54.2	348.7	35.8	4.1
Site NM14 (31°35′12.7″N, 91°22′11.1″E)							
NM14-2A	294/31	4	328.7	44.9	343.4	26.5	6.6
NM14-3A	294/31	6	329.4	46.6	344.7	27.8	3.5
NM14-4A	294/31	6	324.0	45.3	340.3	28.3	4.0
NM14-5A	294/31	4	334.5	46.8	348.4	26.6	2.4
NM14-6A	294/31	6	327.9	40.9	341.0	23.0	3.3
NM14-7A	294/31	8	333.0	49.6	348.6	29.6	3.4
NM14-8A	294/31	5	328.9	51.0	346.5	31.9	7.6
NM14-9A	294/31	6	322.0	42.1	337.1	26.0	5.3
NM14-10A	294/31	6	326.7	51.5	345.4	33.0	5.9
NM14-11A	294/31	6	331.8	42.1	344.5	23.0	8.9
NM14-12A	294/31	5	310.0	38.6	326.3	27.3	5.1
Site NM15 (31°35′12.7″N, 91°22′11″E)							
NM15-1A	291/30	6	330.8	46.3	346.7	23.9	3.8
NM15-2A	291/30	6	343.3	39.5	352.8	14.2	4.3
NM15-3A	291/30	6	332.4	48.0	348.6	25.0	1.9
NM15-4A	291/30	6	315.3	31.4	327.9	16.7	6.8
NM15-5A	291/30	6	326.9	46.4	344.2	25.4	3.7
NM15-6A	291/30	6	334.4	47.1	349.5	23.6	4.4
NM15-7A	291/30	5	332.7	47.1	348.4	24.2	3.1
NM15-8A	291/30	6	339.7	51.8	355.2	26.5	10.6
NM15-9A	291/30	6	328.4	40.3	342.2	19.4	4.5
NM15-10A	291/30	6	324.7	28.6	333.9	10.3	8.6
Site NM16 (31°35′13.1″N, 91°22′10.3″E)							
NM16-1A	305/28	6	310.6	33.0	324.2	19.4	9.7
NM16-2A	305/28	5	335.9	42.1	347.3	18.6	5.7
NM16-3A	305/28	6	340.9	47.6	353.0	22.4	3.0
NM16-4A	305/28	6	319.4	39.1	333.9	21.2	6.1

NM16-5A	305/28	4	320.7	36.9	333.8	18.7	2.0
NM16-6A	305/28	7	325.8	46.2	342.0	25.3	4.1
NM16-7A	305/28	6	319.5	38.6	333.8	20.7	4.2
NM16-8A	305/28	6	316.6	39.2	331.9	22.3	6.4
NM16-9A	305/28	6	353.8	65.1	7.1	36.8	3.2
NM16-10A	305/28	5	319.4	29.9	329.5	13.0	9.7
Site NM17 (31°35′13.5″N, 91°22′10.8″E)							
NM17-1A	299/27	6	321.0	54.4	348.1	39.9	3.5
NM17-2A	299/27	5	326.9	47.7	347.3	32.4	3.8
NM17-3A	299/27	4	331.3	54.5	354.5	36.7	2.7
NM17-5A	299/27	5	332.6	58.4	357.9	39.7	3.8
NM17-6A	299/27	4	326.3	56.5	352.9	40.0	5.2
NM17-7A	299/27	5	323.0	62.8	356.3	45.9	2.6
NM17-8A	299/27	4	321.3	59.2	352.1	43.7	3.0
NM17-9A	299/27	6	322.2	58.6	352.2	42.9	1.0
NM17-10A	299/27	7	323.5	54.1	349.4	38.9	1.5
Site NM18 (31°35′13.6″N, 91°22′10.8″E)							
NM18-1A	303/31	7	312.9	50.2	337.0	37.9	2.1
NM18-2A	303/31	7	312.4	43.3	332.1	32.3	3.0
NM18-3A	303/31	7	311.7	48.9	335.2	37.3	3.7
NM18-5A	303/31	7	314.9	44.5	334.7	32.4	2.2
NM18-6A	303/31	6	323.3	50.6	344.3	34.7	5.6
NM18-7A	303/31	6	313.3	46.9	335.1	35.0	2.6
NM18-8A	303/31	5	310.3	48.2	333.8	37.2	3.9
NM18-10A	303/31	7	305.7	46.0	329.0	37.1	1.3
Site NM19 (31°35′14″N, 91°22′11″E)							
NM19-1A	304/20	7	333.9	37.8	347.4	18.4	2.8
NM19-2A	304/20	5	308.0	43.2	332.2	33.6	2.2
NM19-3A	304/20	6	315.1	41.6	336.0	29.2	3.6
NM19-4A	304/20	4	310.1	36.9	329.4	27.6	3.8
NM19-5A	304/20	5	310.6	33.5	327.6	24.6	2.0
NM19-6A	304/20	6	341.8	41.4	354.8	19.0	1.4
NM19-7A	304/20	5	318.9	42.9	339.6	28.7	2.7
NM19-8A	304/20	7	324.7	30.6	336.8	15.8	2.3
NM19-10A	304/20	6	306.3	30.8	322.7	24.4	3.0
Site NM20 (31°35′16.9″N, 91°22′10.3″E)							
NM20-1A	304/20	6	335.1	41.8	346.7	29.7	3.0
NM20-2A	304/20	6	324.8	44.1	339.4	34.5	4.4
NM20-4A	304/20	6	312.2	17.9	317.8	14.0	5.9
NM20-5A	304/20	8	346.0	40.4	355.0	25.8	4.8
NM20-6A	304/20	4	354.1	47.2	3.5	30.7	4.2

NM20-7A	304/20	6	335.5	36.4	345.1	24.4	5.1
NM20-8A	304/20	5	329.3	29.0	337.2	19.2	12.0
NM20-9A	304/20	5	330.8	48.3	346.2	36.8	8.0
NM20-10A	304/20	5	322.6	51.2	341.4	41.6	6.7
Site NM21 (31°35′17.1″N, 91°22′10.2″E)							
NM21-1A	299/29	4	340.9	33.0	349.4	11.8	3.1
NM21-2A	299/29	6	347.2	44.4	358.4	20.7	6.2
NM21-3A	299/29	5	342.1	37.6	352.0	15.7	3.7
NM21-4A	299/29	7	302.3	47.3	329.0	38.6	4.3
NM21-5A	299/29	7	329.9	39.2	343.6	21.1	3.1
NM21-6A	299/29	7	324.4	40.0	339.9	23.8	2.7
NM21-7A	299/29	5	331.5	38.7	344.5	20.1	5.1
NM21-8A	299/29	4	317.9	42.6	336.6	28.4	3.7
NM21-9A	299/29	5	324.3	48.5	344.6	31.1	2.8
NM21-11A	299/29	7	332.2	19.1	336.7	2.1	4.0
Site NM22 (31°35′17.2″N, 91°22′9.5″E)							
NM22-1A	295/33	7	318.3	57.3	347.1	36.1	6.4
NM22-2A	295/33	6	305.8	43.1	329.2	29.9	4.6
NM22-3A	295/33	6	325.0	50.9	346.6	28.7	3.3
NM22-4A	295/33	5	344.4	54.9	0.3	26.6	3.0
NM22-5A	295/33	5	302.8	49.6	332.3	36.2	4.8
NM22-6A	295/33	5	319.2	41.0	336.9	22.4	4.0
NM22-7A	295/33	7	316.0	43.9	336.5	26.2	2.5
NM22-8A	295/33	7	325.2	46.0	343.7	24.4	1.3
NM22-9A	295/33	5	314.7	44.9	336.2	27.5	1.4
NM22-10A	295/33	4	312.8	48.7	337.6	31.3	4.4
Site NM23 (31°35′17.6″N, 91°22′9.7″E)							
NM23-1A	299/28	5	337.2	40.8	349.4	20.9	2.0
NM23-2A	299/28	8	326.3	52.8	348.1	35.0	2.1
NM23-3A	299/28	7	325.4	45.7	343.2	29.1	1.5
NM23-4A	299/28	7	318.7	34.9	332.6	22.1	2.1
NM23-5A	299/28	7	329.1	39.6	342.9	22.4	2.1
NM23-6A	299/28	7	318.8	43.2	337.1	29.2	1.5
NM23-7A	299/28	7	332.3	42.2	346.4	23.7	3.9
NM23-8A	299/28	7	320.9	41.7	337.9	27.2	5.2
NM23-9A	299/28	7	311.3	47.0	334.2	35.3	4.1
NM23-10A	299/28	7	330.1	57.8	353.5	38.1	3.5
Site NM24 (31°35′18″N, 91°22′9.3″E)							
NM24-1A	300/24	7	316.5	47.7	336.4	36.7	2.4
NM24-3A	300/24	5	327.4	38.9	340.2	25.3	2.4
NM24-4A	300/24	5	321.9	42.4	337.5	30.3	2.0

NM24-5A	300/24	7	332.4	44.9	346.7	29.4	1.6
NM24-6A	300/24	6	318.5	39.7	333.5	29.0	1.4
NM24-7A	300/24	5	318.9	41.9	334.9	30.8	1.7
NM24-8A	300/24	4	323.2	49.4	342.2	36.1	2.7
NM24-9A	300/24	5	312.7	54.1	338.0	43.4	3.7
NM24-10A	300/24	7	324.2	45.3	340.8	32.2	4.7
NM24-11A	300/24	6	327.4	49.3	345.2	34.8	2.9
Site NM25 (31°35′18.5″N, 91°22′8.9″E)							
NM25-1A	298/21	7	316.8	26.8	325.0	18.6	2.2
NM25-2A	298/21	6	327.0	34.0	336.5	22.2	4.8
NM25-3A	298/21	5	316.9	45.3	333.1	35.6	5.1
NM25-4A	298/21	7	339.4	33.8	346.8	18.8	5.8
NM25-5A	298/21	6	330.9	42.9	343.0	29.6	2.0
NM25-6A	298/21	5	313.1	45.6	330.3	37.0	6.0
NM25-7A	298/21	6	317.1	45.4	333.3	35.6	3.6
NM25-8A	298/21	5	324.3	36.7	335.2	25.5	5.7
NM25-9A	298/21	6	319.7	33.3	330.0	23.7	3.2
NM25-10A	298/21	6	332.6	44.1	344.8	30.3	3.5
Site NM26 (31°35′19.2″N, 91°22′9″E)							
NM26-1A	293/27	6	328.2	49.5	345.0	30.5	5.0
NM26-2A	293/27	7	322.1	38.9	335.4	22.9	3.6
NM26-3A	293/27	6	321.0	38.3	334.4	22.7	3.5
NM26-4A	293/27	5	322.1	39.4	335.7	23.3	4.5
NM26-5A	293/27	6	324.7	45.9	340.7	28.3	5.9
NM26-6A	293/27	6	317.3	43.0	333.9	28.1	3.5
NM26-7A	293/27	5	316.3	39.8	331.5	25.7	3.9
NM26-8A	293/27	4	328.9	53.3	347.4	33.7	3.3
NM26-9A	293/27	6	321.9	40.3	335.9	24.1	1.8
NM26-10A	293/27	5	333.6	52.9	350.2	32.2	5.0
Site NM27 (31°35′19.5″N, 91°22′8.8″E)							
NM27-1A	306/36	6	330.7	37.2	346.8	17.1	3.4
NM27-2A	306/36	7	329.5	35.0	344.7	15.8	1.6
NM27-3A	306/36	4	308.6	52.6	344.9	38.8	4.6
NM27-4A	306/36	6	324.7	34.6	341.1	17.7	3.6
NM27-5A	306/36	5	336.1	32.6	348.1	10.8	7.0
NM27-6A	306/36	7	0.6	54.2	14.5	22.1	6.2
NM27-7A	306/36	7	338.4	39.6	353.4	15.8	6.9
NM27-8A	306/36	6	322.7	30.0	336.8	14.9	4.4
NM27-9A	306/36	6	327.3	43.7	348.6	23.9	9.1
NM27-11A	306/36	6	325.3	54.2	354.9	32.8	6.5
Site NM28 (31°35′19.6″N, 91°22′8.9″E)							

NM28-1A	299/38	7	326.8	39.5	343.7	16.2	4.1
NM28-2A	299/38	6	328.9	46.5	349.2	21.1	6.3
NM28-3A	299/38	5	343.7	59.4	5.0	27.3	10.2
NM28-4A	299/38	6	332.6	36.3	345.9	11.1	3.3
NM28-5A	299/38	5	327.5	40.9	345.0	17.1	8.6
NM28-6A	299/38	6	310.2	37.2	331.3	22.4	5.2
NM28-7A	299/38	5	326.0	49.3	349.3	24.6	3.1
NM28-8A	299/38	5	322.1	39.6	340.6	18.4	2.3
NM28-9A	299/38	7	323.8	30.3	336.2	10.1	5.3
NM28-10A	299/38	5	324.1	46.2	346.2	22.9	3.4
Site NM29 (31°35′19.8″N, 91°22′8.7″E)							
NM29-1A	301/25	5	323.1	45.1	340.6	32.0	6.9
NM29-2A	301/25	7	339.2	37.2	349.3	19.9	2.7
NM29-3A	301/25	6	341.4	39.3	351.8	21.2	7.2
NM29-4A	301/25	5	326.4	42.3	341.6	28.4	10.7
NM29-5A	301/25	5	339.7	41.8	351.4	24.1	6.1
NM29-6A	301/25	5	317.3	41.6	334.3	30.9	4.0
NM29-7A	301/25	6	315.3	42.9	333.4	32.7	2.1
NM29-8A	301/25	6	321.3	42.4	337.7	30.2	4.0
NM29-9A	301/25	5	323.9	37.0	337.1	24.4	4.2
NM29-10A	301/25	6	336.6	58.6	357.3	40.2	9.1
Site NM30 (31°35′20.5″N, 91°22′10.2″E)							
NM30-1A	291/33	6	316.9	30.0	328.1	12.4	5.1
NM30-2A	291/33	5	322.6	30.8	332.9	10.6	4.2
NM30-3A	291/33	5	334.5	34.6	343.7	9.6	4.3
NM30-4A	291/33	4	312.3	42.4	331.7	24.8	7.6
NM30-5A	291/33	7	334.3	53.3	351.9	26.7	9.2
NM30-6A	291/33	7	328.1	30.6	337.0	8.3	4.3
NM30-7A	291/33	6	336.2	45.3	349.4	18.9	8.9
NM30-8A	291/33	5	335.7	34.3	344.5	9.0	7.0
NM30-9A	291/33	6	326.7	26.3	334.0	4.9	5.8
NM30-10A	291/33	5	327.7	48.4	345.3	24.2	4.2
NM30-11A	291/33	4	322.5	50.5	343.2	27.8	7.4
Site NM31 (31°35′20.9″N, 91°22′10.4″E)							
NM31-1A	294/25	6	318.8	36.3	331.3	23.2	8.4
NM31-2A	294/25	5	327.8	42.2	340.9	25.7	7.5
NM31-3A	294/25	6	324.1	28.9	332.5	14.6	4.6
NM31-4A	294/25	5	1.7	39.0	6.2	15.5	8.3
NM31-5A	294/25	6	318.1	43.1	334.0	29.5	6.5
NM31-6A	294/25	5	331.1	51.6	347.5	33.5	4.0
NM31-7A	294/25	5	324.2	35.0	335.0	20.3	6.2

Site NM32 (31°34′53.9″N, 91°22′26.1″E)							
NM32-1A	272/41	5	54.7	66.9	23.7	32.6	4.1
NM32-2A	272/41	4	357.6	60.4	359.7	19.5	4.3
NM32-3A	272/41	5	356.3	67.3	359.6	26.4	2.3
NM32-4A	272/41	4	301.7	76.5	346.3	41.1	5.6
NM32-5A	272/41	6	316.9	56.7	337.2	22.1	4.4
NM32-6A	272/41	6	283.6	57.7	322.5	34.5	5.3
NM32-7A	272/41	4	297.2	76.5	345.5	42.0	4.7
NM32-8A	272/41	5	326.1	48.5	338.6	12.4	5.3
NM32-9A	272/41	6	344.7	54.5	351.7	14.5	3.3
NM32-10A	272/41	6	332.7	53.2	344.3	15.2	3.7
Site NM33 (31°34′54″N, 91°22′25.8″E)							
NM33-1A	278/47	4	302.9	59.4	337.2	25.5	11.7
NM33-2A	278/47	8	308.8	56.3	337.3	21.1	3.3
NM33-3A	278/47	6	291.1	61.2	334.7	31.2	5.9
NM33-4A	278/47	5	313.0	52.1	336.4	16.2	7.6
NM33-5A	278/47	5	298.1	78.5	354.2	38.2	5.9
NM33-6A	278/47	5	301.2	67.7	343.9	31.4	3.9
NM33-7A	278/47	6	306.4	63.7	342.0	27.2	3.6
NM33-8A	278/47	6	343.1	63.4	356.5	18.2	3.6
NM33-9A	278/47	4	290.3	60.3	333.6	31.0	4.9
NM33-10A	278/47	4	290.7	62.8	336.2	32.2	7.7
Site NM34 (31°34′54.1″N, 91°22′25.8″E)							
NM34-1A	276/48	4	305.6	63.1	340.1	25.5	3.7
NM34-2A	276/48	7	295.9	57.6	332.1	25.4	2.0
NM34-3A	276/48	5	305.7	65.5	342.1	27.1	2.8
NM34-4A	276/48	6	319.0	48.6	336.7	9.6	2.3
NM34-5A	276/48	4	311.1	59.6	339.6	21.1	2.4
NM34-6A	276/48	6	298.8	65.1	339.6	29.0	3.5
NM34-7A	276/48	6	306.1	70.5	346.4	30.4	2.4
NM34-8A	276/48	5	301.9	50.0	328.6	17.7	4.2
NM34-9A	276/48	5	300.0	57.2	333.3	23.5	3.9
NM34-10A	276/48	7	310.9	48.1	331.9	12.4	2.4
Site NM35 (31°34′54.1″N, 91°22′25.8″E)							
NM35-1A	276/48	4	294.7	71.9	345.2	34.2	7.0
NM35-2A	276/48	5	296.9	72.8	346.5	34.1	7.5
NM35-3A	276/48	4	289.4	58.7	330.8	28.8	4.5
NM35-4A	276/48	4	299.4	49.4	327.0	18.4	5.2
NM35-5A	276/48	7	307.1	57.5	336.5	21.0	3.4
NM35-6A	276/48	4	306.6	63.9	341.2	25.8	2.8
NM35-7A	276/48	5	305.3	54.5	333.5	19.5	4.0

NM35-9A	276/48	5	299.0	56.9	332.7	23.7	3.8
NM35-10A	276/48	6	318.2	60.1	343.0	19.3	7.8
NM35-11A	276/48	4	306.3	64.6	341.6	26.4	5.8
Site NM36 (31°34′54.2″N, 91°22′25.8″E)							
NM36-1A	276/48	7	302.8	54.5	332.4	20.5	3.3
NM36-2A	276/48	6	311.2	54.3	336.1	17.1	1.8
NM36-3A	276/48	6	302.4	47.2	326.8	15.4	1.8
NM36-5A	276/48	6	321.6	65.2	347.4	22.6	3.6
NM36-6A	276/48	6	343.4	60.6	354.8	14.3	5.9
NM36-7A	276/48	6	296.5	55.9	330.9	24.1	2.7
NM36-8A	276/48	6	327.9	59.8	347.1	16.5	4.5
NM36-9A	276/48	4	276.7	55.4	323.3	33.0	3.1
NM36-10A	276/48	6	311.7	60.8	340.7	21.9	4.3
NM36-11A	276/48	6	321.2	67.7	348.9	24.8	4.7
Site NM37 (31°34′54.4″N, 91°22′24.9″E)							
NM37-1A	279/32	5	312.9	50.5	332.3	27.8	2.5
NM37-2A	279/32	6	316.5	65.9	344.0	40.0	5.6
NM37-3A	279/32	7	303.8	51.9	327.6	32.0	2.2
NM37-4A	279/32	7	340.5	60.7	353.2	30.8	2.5
NM37-5A	279/32	7	325.5	55.4	342.6	28.7	1.8
NM37-6A	279/32	5	288.8	64.2	330.6	46.4	3.5
NM37-7A	279/32	5	303.4	56.6	330.7	36.0	1.4
NM37-8A	279/32	6	311.4	53.7	333.3	31.0	2.8
NM37-9A	279/32	4	294.0	49.1	319.7	33.5	5.8
NM37-10A	279/32	4	321.0	62.6	343.9	36.2	1.9
Site NM38 (31°34′54.4″N, 91°22′24.8″E)							
NM38-1A	279/32	7	313.0	54.3	334.6	31.0	2.3
NM38-2A	279/32	6	308.2	40.8	324.0	21.0	4.7
NM38-3A	279/32	6	316.4	52.1	335.4	28.1	2.2
NM38-4A	279/32	5	319.0	59.7	341.2	34.1	1.6
NM38-5A	279/32	5	306.2	70.8	344.0	46.2	1.3
NM38-6A	279/32	7	294.5	50.2	320.8	34.1	4.6
NM38-7A	279/32	5	329.4	40.3	338.9	13.7	4.8
NM38-8A	279/32	7	322.7	67.7	348.0	40.2	3.0
NM38-10A	279/32	4	335.7	56.9	349.2	27.9	3.3
NM38-11A	279/32	5	318.7	59.2	340.7	33.7	1.9
Site NM39 (31°34′54.6″N, 91°22′24.9″E)							
NM39-1A	273/36	5	266.5	48.5	303.0	40.6	3.7
NM39-2A	273/36	5	288.9	66.8	331.8	42.8	4.1
NM39-3A	273/36	4	342.8	53.7	350.6	19.0	2.9
NM39-4A	273/36	5	315.8	52.5	333.8	23.5	2.8

NM39-5A	273/36	6	302.2	57.4	329.4	31.8	2.8
NM39-6A	273/36	6	335.4	46.5	343.9	13.1	1.4
NM39-7A	273/36	6	332.6	61.7	347.2	28.1	5.1
NM39-8A	273/36	6	308.1	61.3	335.0	33.2	2.4
NM39-9A	273/36	4	1.4	66.1	2.2	30.1	10.8
NM39-10A	273/36	4	307.0	59.6	333.3	32.1	4.6
Site NM40 (31°34′54.7″N, 91°22′23.9″E)							
NM40-1A	272/40	7	311.3	56.0	333.7	24.1	3.2
NM40-2A	272/40	4	326.3	51.7	339.9	16.1	2.7
NM40-4A	272/40	6	302.7	48.6	324.5	21.0	3.3
NM40-5A	272/40	4	303.2	48.7	324.8	20.8	6.4
NM40-6A	272/40	5	319.1	50.7	335.2	17.1	4.3
NM40-7A	272/40	5	306.8	74.7	345.6	39.9	3.1
NM40-8A	272/40	4	326.3	54.5	341.1	18.7	4.9
NM40-9A	272/40	7	320.5	56.5	338.8	21.9	2.6
NM40-10A	272/40	5	307.5	54.9	331.1	24.3	2.9
Site NM41 (31°34′55″N, 91°22′24.4″E)							
NM41-1A	269/31	6	325.7	68.5	343.8	39.8	1.9
NM41-2A	269/31	6	303.9	65.0	331.8	40.7	3.3
NM41-3A	269/31	6	304.5	51.9	323.8	29.4	3.5
NM41-4A	269/31	4	294.3	62.2	325.1	41.0	2.1
NM41-5A	269/31	5	310.6	70.4	338.6	43.9	1.9
NM41-6A	269/31	5	298.8	68.2	332.1	44.5	1.9
NM41-7A	269/31	5	323.0	58.1	337.9	30.5	2.9
NM41-8A	269/31	4	328.6	59.4	341.6	30.8	1.6
NM41-9A	269/31	5	329.5	59.8	342.2	31.0	2.2
NM41-10A	269/31	7	325.3	52.8	337.3	25.1	2.6
Site NM42 (31°34′55″N, 91°22′24.6″E)							
NM42-1A	281/48	5	330.3	55.9	348.9	13.8	5.3
NM42-2A	281/48	5	357.0	65.4	4.9	18.0	9.4
NM42-3A	281/48	5	313.9	48.1	335.9	13.2	5.0
NM42-4A	281/48	5	311.7	58.1	341.7	21.5	1.4
NM42-5A	281/48	7	306.6	47.7	331.8	16.2	2.3
NM42-7A	281/48	7	312.7	54.4	339.5	18.4	2.2
NM42-8A	281/48	5	315.9	57.3	343.0	19.5	6.9
NM42-9A	281/48	4	339.1	63.4	356.5	18.4	5.2
NM42-10A	281/48	5	297.9	56.9	335.3	26.2	4.7
Site NM43 (31°34′55.1″N, 91°22′24.5″E)							
NM43-1A	269/49	5	314.3	54.5	334.2	12.8	3.2
NM43-2A	269/49	4	321.9	56.2	338.9	12.2	5.0
NM43-4A	269/49	4	308.2	56.0	332.2	16.1	1.4

NM43-5A	269/49	5	322.5	58.9	340.5	14.3	5.5
NM43-6A	269/49	6	333.5	60.8	346.5	13.9	4.5
NM43-7A	269/49	5	307.7	51.9	329.4	13.0	5.1
NM43-8A	269/49	5	289.2	35.1	307.9	9.5	3.6
NM43-9A	269/49	6	328.0	56.9	342.3	11.3	4.0
NM43-10A	269/49	7	329.2	56.1	342.6	10.3	3.0
Site NM44 (31°34′55.1″N, 91°22′24.5″E)							
NM44-2A	269/49	4	313.7	53.4	333.3	12.1	5.6
NM44-3A	269/49	4	291.0	68.9	336.2	30.7	7.2
NM44-4A	269/49	5	316.8	56.6	336.6	13.9	4.9
NM44-5A	269/49	4	311.5	61.4	337.0	19.4	2.9
NM44-6A	269/49	5	307.4	53.6	330.3	14.5	6.5
NM44-7A	269/49	4	297.8	68.3	337.4	28.3	1.9
NM44-8A	269/49	6	325.3	65.2	344.7	19.4	5.6
NM44-9A	269/49	6	316.7	59.9	338.4	16.7	3.5
NM44-10A	269/49	5	313.6	57.9	335.9	15.9	5.9
Site NM45 (31°34′55.2″N, 91°22′24.5″E)							
NM45-1A	263/34	7	309.0	61.6	329.9	32.5	4.4
NM45-2A	263/34	6	286.3	61.8	319.2	38.8	2.4
NM45-3A	263/34	7	309.4	63.3	331.1	34.0	2.5
NM45-4A	263/34	6	302.7	60.1	325.9	32.7	2.9
NM45-5A	263/34	6	300.0	61.6	325.4	34.7	4.2
NM45-6A	263/34	5	303.6	63.0	328.1	35.0	3.8
NM45-7A	263/34	5	301.7	73.6	335.1	44.1	5.1
NM45-8A	263/34	4	291.8	61.5	321.5	36.9	4.6
NM45-9A	263/34	6	281.7	71.2	326.6	46.6	3.0
NM45-10A	263/34	6	297.1	73.2	333.3	44.6	2.4
Site NM46 (31°34′55.2″N, 91°22′24.5″E)							
NM46-1A	263/34	5	304.8	47.6	320.4	21.2	7.1
NM46-3A	263/34	8	290.9	63.3	322.5	38.6	1.8
NM46-4A	263/34	5	298.3	65.1	327.1	38.0	2.6
NM46-5A	263/34	5	276.0	68.5	321.7	46.5	3.3
NM46-6A	263/34	5	276.3	63.7	316.6	43.3	2.6
NM46-7A	263/34	5	307.4	58.9	327.6	30.5	2.4
NM46-8A	263/34	6	304.3	57.8	325.4	30.3	3.1
NM46-9A	263/34	7	288.5	50.5	311.9	29.1	4.5
NM46-10A	263/34	4	312.7	65.8	334.0	35.5	9.3
Site NM47 (31°34′55.3″N, 91°22′24.5″E)							
NM47-1A	267/42	5	241.0	74.6	333.9	52.6	6.6
NM47-2A	267/42	6	70.1	81.8	8.1	45.1	3.6
NM47-4A	267/42	6	301.5	51.7	324.0	20.4	4.3

NM47-5A	267/42	6	291.0	57.5	323.0	28.7	5.9
NM47-6A	267/42	4	267.3	52.6	308.4	36.1	6.7
NM47-7A	267/42	6	309.0	64.6	335.7	28.6	4.6
NM47-8A	267/42	8	268.7	57.5	314.0	38.0	1.9
NM47-9A	267/42	5	301.1	55.1	326.0	23.3	3.4
NM47-10A	267/42	6	283.6	67.3	329.1	37.7	4.8
Site NM48 (31°34′55.3″N, 91°22′24.5″E)							
NM48-1A	267/42	5	285.0	66.3	328.5	36.7	6.2
NM48-2A	267/42	5	278.5	56.2	316.5	32.9	1.9
NM48-3A	267/42	4	304.7	51.2	325.4	18.8	6.6
NM48-5A	267/42	4	302.3	55.5	326.8	23.2	4.4
NM48-6A	267/42	5	288.3	61.4	325.1	32.4	2.4
NM48-7A	267/42	6	281.8	57.0	318.7	32.0	3.8
NM48-9A	267/42	5	272.0	51.9	309.7	33.3	3.7
NM48-10A	267/42	4	274.5	51.3	310.3	31.7	2.5
Site NM49 (31°34′55.9″N, 91°22′24.7″E)							
NM49-1A	307/43	6	306.1	57.4	353.5	38.4	5.7
NM49-2A	307/43	5	337.4	59.9	7.9	27.3	5.9
NM49-3A	307/43	5	302.9	70.0	8.2	44.7	4.9
NM49-4A	307/43	5	310.3	54.7	352.2	35.1	2.6
NM49-5A	307/43	5	287.6	60.7	352.8	48.5	8.5
NM49-6A	307/43	4	331.4	67.0	11.5	34.2	6.1
NM49-7A	307/43	4	297.5	60.3	354.5	43.7	11.7
NM49-8A	307/43	5	297.6	67.1	3.6	45.8	5.0
NM49-9A	307/43	5	340.3	61.5	10.2	27.6	7.8
NM49-10A	307/43	5	305.0	49.2	344.4	34.6	5.5
Site NM50 (31°34′55.9″N, 91°22′24.9″E)							
NM50-1A	307/37	4	302.1	37.5	328.6	31.9	6.1
NM50-2A	307/37	5	302.5	71.4	7.0	50.5	9.3
NM50-3A	307/37	4	296.7	45.1	332.1	39.9	10.0
NM50-5A	307/37	5	296.1	62.6	352.9	49.6	4.9
NM50-6A	307/37	5	332.4	54.0	359.3	29.6	3.5
NM50-7A	307/37	5	314.7	46.1	343.4	31.3	5.8
NM50-8A	307/37	4	301.1	68.0	1.8	49.8	4.4
NM50-9A	307/37	5	318.6	52.9	351.3	34.3	3.5

Note: N—number of consecutive demagnetization steps used to define the HTC direction; D_g/I_g—declination and inclination in geographic coordinates; D_s/I_s—declination and inclination in stratigraphic coordinates; MAD—mean angular deviation of the HTC fit.

TABLE S4. SUMMARY OF THE AVAILABLE CRETACEOUS PALEOMAGNETIC RESULTS FROM THE SHIQUANHE, GERZE, CUOQIN, MAXIANG, LINZHOU, AND NAQU AREAS IN THE LHASA TERRANE.

Site ID	Locality		D_s	I_s	Paleopole		Reference point		D_r	I_r
	Slat (°)	Slong (°)	(°)	(°)	Plat (°)	Plong (°)	Rlat (°)	Rlong (°)	(°)	(°)
Shiquanhe area										
The Early Cretaceous (~116–113 Ma) Zenong Group volcanic rocks and Jiega Formation limestone results reported by Bian et al. (2017).										
D1	32.2	80.4	343.9	41.7	73.6	324.4	32.3	80.4	343.9	41.8
D2	32.2	80.4	335.4	33.1	63.7	323.8	32.3	80.4	335.4	33.2
D3	32.2	80.4	341.3	40.0	71.0	325.4	32.3	80.4	341.3	40.2
D4	32.2	80.4	333.6	40.5	65.0	335.8	32.3	80.4	333.6	40.6
D5	32.2	80.4	337.4	33.5	65.4	321.5	32.3	80.4	337.4	33.7
D6	32.2	80.4	326.2	31.4	55.9	332.0	32.3	80.4	326.2	31.5
D7	32.2	80.4	334.8	35.4	64.1	327.3	32.3	80.4	334.8	35.5
D8	32.2	80.4	331.9	38.0	62.8	333.9	32.3	80.4	331.9	38.1
D9	32.2	80.4	338.6	39.7	68.7	328.7	32.3	80.4	338.6	39.8
D10	32.2	80.4	332.0	36.1	62.2	331.4	32.3	80.4	332	36.3
D11	32.2	80.4	335.1	34.3	64.0	325.6	32.3	80.4	335.1	34.5
D12	32.2	80.4	330.6	33.1	60.0	329.4	32.3	80.4	330.6	33.2
D13	32.2	80.4	343.1	32.9	69.1	311.3	32.3	80.4	343.1	33.0
T1	32.2	80.4	352.9	39.6	78.4	295.5	32.3	80.4	352.8	39.8
T2	32.2	80.4	354.0	19.4	67.1	276.1	32.3	80.4	353.9	19.6
T3	32.2	80.4	324.8	31.3	54.7	333.6	32.3	80.4	324.6	31.7
T4	32.2	80.4	0.4	36.6	78.2	259.0	32.3	80.4	0.3	36.8
T5	32.2	80.4	0.1	33.7	76.2	260.4	32.3	80.4	360	33.8
T6	32.2	80.4	4.0	43.4	82.3	232.9	32.3	80.4	3.9	43.5
The Late Cretaceous (~92.5 Ma) volcanic results reported by Yi et al. (2015).										
xa161	32.4	80.1	27.9	32.2	60.8	193.9	32.3	80.4	28.0	32.4
xa162	32.4	80.1	20.8	32.1	66.0	203.5	32.3	80.4	20.9	32.2
xa163	32.4	80.1	9.9	34.2	73.8	224.4	32.3	80.4	10.0	34.3
xa164	32.4	80.1	0.2	33.6	76.0	259.2	32.3	80.4	0.3	33.5
xa166	32.4	80.1	349.6	38.4	75.8	303.3	32.3	80.4	349.7	38.2
xa172	32.4	80.1	218.5	-25.1	50.0	189.7	32.3	80.4	38.6	25.3
xa176	32.4	80.1	213.7	-19.5	51.7	198.2	32.3	80.4	33.8	19.6
xa181	32.4	80.1	203.9	-12.4	55.7	214.5	32.3	80.4	24.0	12.5
xa182	32.4	80.1	28.4	22	56.5	202.4	32.3	80.4	28.5	22.0
xa183	32.4	80.1	28.6	11	52.2	209.1	32.3	80.4	28.7	11.2
The Late Cretaceous (~68 Ma) Dianzhong Formation volcanic results reported by Ma et al. (2017).										
G1	32.3	80.1	37.1	8.2	45.3	201.4	32.3	80.4	37.2	8.4
G2	32.3	80.1	35.4	39.7	57.3	178.5	32.3	80.4	35.4	39.9
G3	32.3	80.1	46.7	17.2	40.9	188.1	32.3	80.4	46.8	17.5
G4	32.3	80.1	52.6	35	41.4	172.2	32.3	80.4	52.7	35.3
G5	32.3	80.1	51.7	28.8	40.3	177.3	32.3	80.4	51.8	29.1
G6	32.3	80.1	43.5	22.9	45.2	187.1	32.3	80.4	43.6	23.0
G7	32.3	80.1	49.1	35.6	44.5	173.7	32.3	80.4	49.2	35.9
G8	32.3	80.1	39.2	32.9	52	182.7	32.3	80.4	39.3	33.1
G9	32.3	80.1	41.9	31.7	49.3	181.7	32.3	80.4	42.0	31.9
G10	32.3	80.1	45.9	34	46.7	177.1	32.3	80.4	46.0	34.2
G11	32.3	80.1	41.8	36.2	50.8	177.8	32.3	80.4	41.9	36.3
G12	32.3	80.1	45.2	41.2	49.5	170.7	32.3	80.4	45.2	41.4
G13	32.3	80.1	43	39	50.7	174.2	32.3	80.4	43.1	39.2
G15	32.3	80.1	16.5	12.7	59.9	225.9	32.3	80.4	16.6	12.8
G16	32.3	80.1	61.4	32.5	33.2	169.2	32.3	80.4	61.5	32.9
G17	32.3	80.1	14.8	30.3	69.1	216.7	32.3	80.4	14.9	30.4

G18	32.3	80.1	71.9	24.1	21.9	168.7	32.3	80.4	72.0	24.5
The mid-Cretaceous (~113–72 Ma) Jiega Formation limestone results reported by Ma et al. (2018).										
JG1	32.2	80.8	11.3	31.5	64.8	202.4	32.3	80.4	22.2	31.5
JG2	32.2	80.8	7.1	34.8	69.2	205.2	32.3	80.4	18.0	34.8
JG3	32.2	80.8	2.0	27.3	68.7	224.0	32.3	80.4	12.9	27.4
JG4	32.2	80.8	191.3	-49.8	-70.9	349.6	32.3	80.4	22.3	49.8
JG5	32.2	80.8	3.9	25.2	66.6	221.7	32.3	80.4	14.8	25.1
JG6	32.2	80.8	3.5	31.1	69.8	217.0	32.3	80.4	14.4	31.2
JG7	32.2	80.8	186.6	-18.1	-61.9	41.5	32.3	80.4	17.4	18.1
JG8	32.2	80.8	23.3	28.6	62.9	203.8	32.3	80.4	23.2	28.7
JG9	32.2	80.8	24.2	29.5	62.6	201.7	32.3	80.4	24.1	29.5
JG10	32.2	80.8	17.7	26.8	65.9	214.7	32.3	80.4	17.6	27.0
JG11	32.2	80.8	14.8	26.2	67.3	220.9	32.3	80.4	14.7	26.4
JG12	32.2	80.8	15.9	26.7	66.9	218.2	32.3	80.4	15.8	26.9
JG13	32.2	80.8	11.2	26.3	69.1	228.9	32.3	80.4	11.1	26.5
JG14	32.2	80.8	20.8	30.7	65.5	205.6	32.3	80.4	20.7	30.7
JG15	32.2	80.8	17.6	31.6	68.1	210.1	32.3	80.4	17.5	31.6
JG16	32.2	80.8	28.7	38.4	62.4	186.2	32.3	80.4	28.6	38.3
JG17	32.2	80.8	20.3	33.4	67.0	203.3	32.3	80.4	20.2	33.3
JG18	32.2	80.8	25.7	34.3	63.3	194.6	32.3	80.4	25.6	34.2
JG19	32.2	80.8	9.3	35.1	74.7	225.5	32.3	80.4	9.2	35.2
JG20	32.2	80.8	17.1	33.2	69.1	209.1	32.3	80.4	17.0	33.2
JG21	32.2	80.8	20.4	21.0	61.6	214.8	32.3	80.4	20.2	21.0
JG22	32.2	80.8	16.6	29.4	67.7	214.4	32.3	80.4	16.5	29.4
JG23	32.2	80.8	12.9	28.8	69.5	222.9	32.3	80.4	12.8	28.9
JG24	32.2	80.8	13.1	24.9	67.4	225.7	32.3	80.4	13.0	24.9
JG25	32.2	80.8	17.5	37.8	70.9	201.7	32.3	80.4	17.4	37.8
JG26	32.2	80.8	14.2	30.7	69.7	218.1	32.3	80.4	14.1	30.7
JG27	32.2	80.8	200.8	-29.3	-64.9	27.1	32.3	80.4	20.7	29.2
JG28	32.2	80.8	199.4	-36.8	-69.1	20.1	32.3	80.4	19.3	36.8
JG30	32.2	80.8	14.9	31.2	69.6	216.0	32.3	80.4	14.8	31.2
JG31	32.2	80.8	22.9	30.6	64.0	202.5	32.3	80.4	22.8	30.6
JG32	32.2	80.8	22.2	22.7	61.2	210.7	32.3	80.4	22.0	22.7
JG33	32.2	80.8	198.0	-31.0	-67.5	30.1	32.3	80.4	17.9	30.9
JG34	32.2	80.8	18.0	27.4	65.9	213.7	32.3	80.4	17.9	27.4
JG35	32.2	80.8	24.7	27.2	61.3	203.3	32.3	80.4	24.6	27.1
JG36	32.2	80.8	17.3	32.9	68.9	209.1	32.3	80.4	17.2	32.9
JG38	32.2	80.8	11.4	36.5	74.3	217.4	32.3	80.4	11.3	36.5
JG39	32.2	80.8	5.9	37.6	77.7	234.1	32.3	80.4	5.8	37.7
JG40	32.2	80.8	359.8	34.3	76.7	261.6	32.3	80.4	359.7	34.6
The inclination-only mean of 84 Cretaceous paleomagnetic sites (groups) from the Shiquanhe area										**31.4± 2.0**
<u>Gerze area</u>										
The Early Cretaceous (~120–106 Ma) Risong Formation red beds and volcanic results reported by Wang et al. (2022).										
WM1	32.4	83.4	67.9	55.4	34.9	149.5	32.4	83.4	67.9	55.4
WM2	32.4	83.4	64.7	45.6	34.4	160.8	32.4	83.4	64.7	45.6
WM3	32.4	83.4	62.1	48.2	37.3	159.3	32.4	83.4	62.1	48.2
WM4	32.4	83.4	66.0	52.1	35.3	153.9	32.4	83.4	66.0	52.1
WM5	32.4	83.4	60.8	49.1	38.7	158.9	32.4	83.4	60.8	49.1
WM6	32.4	83.4	63.0	48.2	36.6	159.0	32.4	83.4	63.0	48.2
WM7	32.4	83.4	55.4	50.1	43.4	159.7	32.4	83.4	55.4	50.1
WM8	32.4	83.4	67.2	46.9	32.8	158.6	32.4	83.4	67.2	46.9
WM9	32.4	83.4	64.4	44.4	34.3	162.0	32.4	83.4	64.4	44.4
WM10	32.4	83.4	55.7	48.6	42.7	161.3	32.4	83.4	55.7	48.6
WM11	32.4	83.4	60.2	46.8	38.5	161.5	32.4	83.4	60.2	46.8
WM12	32.4	83.4	56.3	41.9	40.3	167.8	32.4	83.4	56.3	41.9

WM13	32.4	83.4	59.5	41.1	37.4	167.0	32.4	83.4	59.5	41.1
WM14	32.4	83.4	60.4	37.2	35.5	169.7	32.4	83.4	60.4	37.2
WM15	32.4	83.4	52.5	44.9	44.3	166.6	32.4	83.4	52.5	44.9
WM16	32.4	83.4	55.7	46.4	42.1	163.7	32.4	83.4	55.7	46.4
WM17	32.4	83.4	57.4	46.3	40.7	163.1	32.4	83.4	57.4	46.3
WM18	32.4	83.4	9.8	27.0	69.8	234.9	32.4	83.4	9.8	27.0
WM19	32.4	83.4	354.6	27.8	71.7	280.2	32.4	83.4	354.6	27.8
WM20	32.4	83.4	7.8	38.4	77.2	228.7	32.4	83.4	7.8	38.4
WM21	32.4	83.4	356.4	23.6	69.7	273.6	32.4	83.4	356.4	23.6
WM22	32.4	83.4	354.9	34.9	76.1	283.8	32.4	83.4	354.9	34.9
WM23	32.4	83.4	347.9	30.7	70.7	300.9	32.4	83.4	347.9	30.7
WM24	32.4	83.4	353.5	34.7	75.5	288.6	32.4	83.4	353.5	34.7
WM25	32.4	83.4	358.1	38.2	78.9	272.7	32.4	83.4	358.1	38.2
WM26	32.4	83.4	354.9	36.8	77.3	285.6	32.4	83.4	354.9	36.8
WM27	32.4	83.4	345.1	38.7	73.1	318.5	32.4	83.4	345.1	38.7
WM28	32.4	83.4	355.9	26.6	71.3	275.9	32.4	83.4	355.9	26.6
WM29	32.4	83.4	354.5	26.5	70.9	279.9	32.4	83.4	354.5	26.5
WM30	32.4	83.4	350.4	41.5	78.0	310.5	32.4	83.4	350.4	41.5
WM31	32.4	83.4	359.2	32.5	75.3	266.4	32.4	83.4	359.2	32.5
WM32	32.4	83.4	354.1	20.9	67.7	278.9	32.4	83.4	354.1	20.9
WM33	32.4	83.4	349.6	22.7	67.3	290.7	32.4	83.4	349.6	22.7
WM34	32.4	83.4	357.5	31.4	74.4	272.3	32.4	83.4	357.5	31.4
WM35	32.4	83.4	56.6	55.3	43.7	152.7	32.4	83.4	56.6	55.3
WM36	32.4	83.4	66.0	52.1	35.3	153.9	32.4	83.4	66.0	52.1
WM37	32.4	83.4	56.7	52.4	42.9	156.5	32.4	83.4	56.7	52.4
WM38	32.4	83.4	52.4	53.9	46.7	155.8	32.4	83.4	52.4	53.9
WM39	32.4	83.4	61.7	48.1	37.6	159.6	32.4	83.4	61.7	48.1
WM40	32.4	83.4	62.4	53.7	38.7	153.2	32.4	83.4	62.4	53.7
WM41	32.4	83.4	67.7	53.0	34.3	152.3	32.4	83.4	67.7	53.0
WM42	32.4	83.4	347.6	30.5	70.5	301.4	32.4	83.4	347.6	30.5
WM43	32.4	83.4	357.2	32.4	75.0	273.8	32.4	83.4	357.2	32.4
WM44	32.4	83.4	353.5	32.6	74.2	286.7	32.4	83.4	353.5	32.6
WM45	32.4	83.4	346.3	24.8	66.9	299.4	32.4	83.4	346.3	24.8
WM46	32.4	83.4	8.6	43.4	79.7	214.5	32.4	83.4	8.6	43.4
WM47	32.4	83.4	357.6	37.3	78.3	274.5	32.4	83.4	357.6	37.3
WM48	32.4	83.4	357.9	37.8	78.6	273.4	32.4	83.4	357.9	37.8
WM49	32.4	83.4	357.8	33.2	75.6	271.8	32.4	83.4	357.8	33.2
WM50	32.4	83.4	353.0	37.1	76.8	293.2	32.4	83.4	353.0	37.1
WM51	32.4	83.4	4.6	32.8	74.9	246.4	32.4	83.4	4.6	32.8
WM52	32.4	83.4	358.4	33.3	75.7	269.6	32.4	83.4	358.4	33.3
WM53	32.4	83.4	357.2	36.3	77.5	275.6	32.4	83.4	357.2	36.3
WM54	32.4	83.4	359.0	39.4	79.9	268.7	32.4	83.4	359.0	39.4
WM55	32.4	83.4	358.5	36.5	77.8	270.1	32.4	83.4	358.5	36.5
WM56	32.4	83.4	358.2	34.6	76.5	270.7	32.4	83.4	358.2	34.6
The inclination-only mean of 56 Early Cretaceous paleomagnetic sites from the Gerze area										**40.2± 3.1**
<u>Cuoqin area</u>										
The Early Cretaceous (~121–117 Ma) Dianzhong Formation volcanic results reported by Yang et al. (2015a).										
DZ14	31.1	84.4	12.0	19.3	66.1	234.1	31.1	84.9	12.2	19.5
DZ15	31.1	84.4	10.0	17.8	66.1	239.3	31.1	84.9	10.2	17.9
DZ17	31.1	84.4	10.4	43.3	79.1	204.6	31.1	84.9	10.5	43.4
DZ18	31.1	84.4	360.0	24.4	71.7	264.4	31.1	84.9	0.2	24.4
DZ19	31.1	84.4	340.5	18.8	61.9	308.7	31.1	84.9	340.7	18.5
DZ20	31.1	84.4	343.0	17.3	62.7	303.4	31.1	84.9	343.2	17.1
DZ21	31.1	84.4	341.5	19.1	62.6	307.2	31.1	84.9	341.7	18.7
DZ22	31.1	84.4	340.4	27.1	65.4	315.8	31.1	84.9	340.5	26.8
DZ23	31.1	84.4	342.9	23.0	65.2	307.7	31.1	84.9	343.1	22.8

DZ24	31.1	84.4	343.9	32.8	70.3	315.9	31.1	84.9	344.0	32.6
DZ25	31.1	84.4	346.3	30.6	70.8	307.9	31.1	84.9	346.5	30.4
DZ26	31.1	84.4	338.0	26.8	63.7	319.3	31.1	84.9	338.2	26.5
The Late Cretaceous (K_2) Jingzhushan Formation red beds results reported by Yang et al. (2015a).										
CQ1	31.2	84.7	308.1	15.9	36.6	340.8	31.1	84.9	308.1	15.8
CQ2	31.2	84.7	309.2	20.1	38.7	342.5	31.1	84.9	309.2	20.0
CQ3	31.2	84.7	313.1	22.6	42.7	341.4	31.1	84.9	313.1	22.6
CQ4	31.2	84.7	310.6	27.2	41.9	346.1	31.1	84.9	310.6	27.1
CQ5	31.2	84.7	308.5	25.4	39.6	346.2	31.1	84.9	308.5	25.2
CQ6	31.2	84.7	300.6	23.2	32.3	349.6	31.1	84.9	300.6	23.2
CQ7	31.2	84.7	308.1	19.7	37.7	343	31.1	84.9	308.1	19.7
CQ8	31.2	84.7	311	18.3	39.7	340.2	31.1	84.9	311.0	18.3
CQ9	31.2	84.7	314.2	26.6	44.8	343.3	31.1	84.9	314.2	26.5
CQ10	31.2	84.7	306.1	26.9	38	348.7	31.1	84.9	306.1	26.8
CQ11	31.2	84.7	311.6	27	42.7	345.3	31.1	84.9	311.6	26.8
CQ12	31.2	84.7	308.4	23.8	39.1	345.3	31.1	84.9	308.4	23.8
CQ13	31.2	84.7	294.3	22.1	26.6	352.4	31.1	84.9	294.3	22.0
CQ14	31.2	84.7	299.8	22.5	31.4	349.6	31.1	84.9	299.8	22.4
CQ15	31.2	84.7	301.7	21.9	32.9	348.2	31.1	84.9	301.7	21.9
CQ16	31.2	84.7	309.1	29.6	41.3	348.7	31.1	84.9	309.1	29.4
CQ17	31.2	84.7	307.3	24.3	38.3	346.3	31.1	84.9	307.3	24.2
CQ18	31.2	84.7	302	16.5	31.6	345	31.1	84.9	302.0	16.4
CQ19	31.2	84.7	301.7	24.9	33.7	349.9	31.1	84.9	301.7	24.7
CQ20	31.2	84.7	296.2	24.3	28.8	352.6	31.1	84.9	296.2	24.1
CQ21	31.2	84.7	338.8	26.8	64.2	318.5	31.1	84.9	338.8	26.7
CQ22	31.2	84.7	324.6	20	51.2	330.2	31.1	84.9	324.7	19.9
CQ23	31.2	84.7	339.1	35.5	67.9	327.7	31.1	84.9	339.2	35.1
CQ24	31.2	84.7	338.5	46.4	71	349.2	31.1	84.9	338.6	46.1
CQ25	31.2	84.7	327.3	46.2	61.4	355.4	31.1	84.9	327.4	45.8
CQ26	31.2	84.7	330.7	50.2	65	1.5	31.1	84.9	330.8	49.8
CQ27	31.2	84.7	332.1	43.1	64.7	347.3	31.1	84.9	332.2	42.7
CQ28	31.2	84.7	330.2	40.3	62.3	344.4	31.1	84.9	330.3	39.8
CQ29	31.2	84.7	338.7	45.4	70.9	346.6	31.1	84.9	338.8	45.0
CQ30	31.2	84.7	338.4	44	70.3	343.7	31.1	84.9	338.5	43.6
CQ31	31.2	84.7	351.4	43.6	80.5	319.4	31.1	84.9	351.5	43.4
CQ32	31.2	84.7	348.8	32	72.8	303.3	31.1	84.9	348.9	31.7
CQ33	31.2	84.7	340	31.1	66.8	320.6	31.1	84.9	340.2	30.7
The Early Cretaceous (~131–110 Ma) Zenong Group volcanic results reported by Chen et al. (2012).										
C15	31.4	85.1	328.3	27.3	56.5	332.1	31.1	84.9	328.3	27.1
C16	31.4	85.1	333.1	32.0	61.9	331.5	31.1	84.9	333.1	31.7
C17	31.4	85.1	333.2	29.0	60.9	328.3	31.1	84.9	333.2	28.8
C18	31.4	85.1	347.7	25.9	69.0	300.4	31.1	84.9	347.6	25.5
C19	31.4	85.1	323.9	39.9	56.9	348.9	31.1	84.9	324.0	39.7
C20	31.4	85.1	145.3	−35.5	56.7	342.9	31.1	84.9	325.3	35.3
DX1	31.4	85.1	317.2	37.1	50.4	350.1	31.1	84.9	317.3	37.0
DX2	31.4	85.1	321.4	29.8	51.7	340.5	31.1	84.9	321.4	29.6
DX3	31.4	85.1	312.6	38.7	46.9	354.3	31.1	84.9	312.6	38.6
DX4	31.4	85.1	316.6	47.2	52.5	2.0	31.1	84.9	316.7	47.1
DX5	31.4	85.1	341.0	36.3	69.6	326.4	31.1	84.9	341.0	36.0
DX6	31.4	85.1	335.8	36.1	65.5	333.4	31.1	84.9	335.8	35.9
DX7	31.4	85.1	323.8	39.7	56.7	348.8	31.1	84.9	323.8	39.6
DX8	31.4	85.1	162.7	−35.9	70.7	322.8	31.1	84.9	342.7	35.6
DX9	31.4	85.1	324.7	37.6	56.9	345.7	31.1	84.9	324.7	37.5
DX10	31.4	85.1	320.2	30.4	50.9	342.0	31.1	84.9	320.2	30.3
DX11	31.4	85.1	307.3	30.2	40.0	350.0	31.1	84.9	307.4	29.9
DX13	31.4	85.1	329.3	44.7	62.7	352.1	31.1	84.9	329.3	44.4
The Late Cretaceous (~93–99 Ma) Dianzhong Fm volcanic results reported by Tang et al. (2013).										

196	31	85	23	13.5	57.7	218.6	31.1	84.9	22.9	13.6
197	31	85	12.3	4.7	59.1	240.6	31.1	84.9	12.2	4.9
198	31	85.1	37.3	33	53.9	187.3	31.1	84.9	37.2	33.0
199	31	85.1	24.6	23.3	60.5	209.4	31.1	84.9	24.5	23.3
200	31	85.2	312.3	8.5	37.9	334.3	31.1	84.9	312.2	9.1
201	31	85.2	331.2	20.6	56.5	324.2	31.1	84.9	331.1	21.1
202	31	85.2	319.6	3.3	41.9	325.7	31.1	84.9	319.5	3.9
203	31	85.2	332.6	-4.4	47.8	308.4	31.1	84.9	332.4	-4.0
204	30.2	85.3	13.9	17.2	64.9	231.2	31.1	84.9	13.8	18.6
205	30.2	85.3	16.2	24.3	67	221.3	31.1	84.9	16.1	25.6
206	30.2	85.3	9	22.5	69.7	239.1	31.1	84.9	8.9	24.0
207	30.2	85.3	10.2	28.5	72.3	231.2	31.1	84.9	10.1	29.8
208	30.2	85.3	12.5	25.9	69.8	227.8	31.1	84.9	12.4	27.2
209	30.2	85.3	11.4	19.5	67.2	235.2	31.1	84.9	11.3	20.9
The inclination-only mean of 77 Cretaceous paleomagnetic sites from the Cuoqin area										**28.3± 3.0**

<u>Maxiang area</u>

The Late Cretaceous (K_2) volcanic and red beds results reported by Sun et al. (2012).

XS1	29.9	90.7	354.7	30.5	75.7	291.7	29.9	90.7	354.7	30.5
XS2	29.9	90.7	342.6	45.1	74.4	352.9	29.9	90.7	342.6	45.1
XS3	29.9	90.7	335.4	27.5	62.7	332.0	29.9	90.7	335.4	27.5
XS4	29.9	90.7	335.2	19.7	59.6	325.4	29.9	90.7	335.2	19.7
XS5	29.9	90.7	345.2	25.0	68.3	313.1	29.9	90.7	345.2	25.0
XS6	29.9	90.7	340.9	46.6	73.2	358.5	29.9	90.7	340.9	46.6
XS7	29.9	90.7	345.4	35.9	73.4	326.9	29.9	90.7	345.4	35.9
XS8	29.9	90.7	2.6	39.2	81.9	253.3	29.9	90.7	2.6	39.2
XS9	29.9	90.7	349.6	41.4	78.9	329.8	29.9	90.7	349.6	41.4
XS10	29.9	90.7	339.7	20.8	63.1	319.6	29.9	90.7	339.7	20.8
XS11	29.9	90.7	336.2	34.5	65.8	339.3	29.9	90.7	336.2	34.5
XS12	29.9	90.7	353.8	27.6	73.7	292.6	29.9	90.7	353.8	27.6
XS13	29.9	90.7	346.5	26.3	69.7	311.5	29.9	90.7	346.5	26.3
XS14	29.9	90.7	339.1	49.0	71.9	6.0	29.9	90.7	339.1	49.0
XS15	29.9	90.7	327.5	46.4	61.5	4.4	29.9	90.7	327.5	46.4
XS16	29.9	90.7	354.7	34.8	78.2	296.0	29.9	90.7	354.7	34.8
XS17	29.9	90.7	339.3	31.0	66.9	330.5	29.9	90.7	339.3	31.0
XS18	29.9	90.7	217.1	-14.9	48.7	205.8	29.9	90.7	37.1	14.9
XS19	29.9	90.7	192.8	-0.9	58.1	245.9	29.9	90.7	12.8	0.9
XS20	29.9	90.7	205.6	-19.6	59.0	215.0	29.9	90.7	25.6	19.6

The Late Cretaceous (~74.2–70.2 Ma) volcanic and red beds results reported by Tong et al. (2022).

MS3-4	29.9	90.7	357.6	9.6	64.9	276.3	29.9	90.7	357.6	9.6
MS5	29.9	90.7	2.7	17.2	68.8	263.3	29.9	90.7	2.7	17.2
MS6	29.9	90.7	1.6	12.2	66.2	266.8	29.9	90.7	1.6	12.2
MS7	29.9	90.7	354.5	10	64.6	283.6	29.9	90.7	354.5	10.0
MS8-10	29.9	90.7	359.1	13.3	66.8	273	29.9	90.7	359.1	13.3
MS11	29.9	90.7	12.8	12.5	63.5	241.1	29.9	90.7	12.8	12.5
MS12	29.9	90.7	353.1	12.9	65.8	287.6	29.9	90.7	353.1	12.9
MS13	29.9	90.7	183.3	–12.8	–66.4	82.5	29.9	90.7	3.3	12.8
MS14	29.9	90.7	193.5	–15.9	–64.8	57.8	29.9	90.7	13.5	15.9
MS16	29.9	90.7	192.3	–17.0	–65.9	59.7	29.9	90.7	12.3	17.0
MS17-18	29.9	90.7	204.5	–22.0	–60.7	34.6	29.9	90.7	24.5	22.0
MS19-20	29.9	90.7	192.4	–27.1	–70.7	51.7	29.9	90.7	12.4	27.1
MS21	29.9	90.7	186.8	–23.7	–71.4	69.5	29.9	90.7	6.8	23.7
MS22	29.9	90.7	191.6	–29.8	–72.5	50.7	29.9	90.7	11.6	29.8
MS23	29.9	90.7	201.9	–26.1	–64.1	34.5	29.9	90.7	21.9	26.1
MS24	29.9	90.7	163	–32.7	–70.4	146.6	29.9	90.7	343	32.7
MS25	29.9	90.7	182.1	–24.3	–72.7	83.8	29.9	90.7	2.1	24.3
MS26	29.9	90.7	36.9	15.3	49	205.7	29.9	90.7	36.9	15.3

MS27	29.9	90.7	156.4	–42.3	–68.4	171.9	29.9	90.7	336.4	42.3
MS28	29.9	90.7	156.9	–16.6	–59.6	140.7	29.9	90.7	336.9	16.6
MS29	29.9	90.7	189.1	–6.4	–62.0	71.1	29.9	90.7	9.1	6.4
MS30	29.9	90.7	183.1	–10.9	–65.4	83.3	29.9	90.7	3.1	10.9
MS31	29.9	90.7	177	–10.7	–65.4	97.9	29.9	90.7	357	10.7
MS32	29.9	90.7	165.5	–10.9	–62.0	122.8	29.9	90.7	345.5	10.9
MS33	29.9	90.7	186.9	–4.5	–61.6	76.1	29.9	90.7	6.9	4.5
MS34	29.9	90.7	193.3	–11.0	–62.6	60.8	29.9	90.7	13.3	11.0
MS35-38	29.9	90.7	191.1	–13.3	–64.6	64.2	29.9	90.7	11.1	13.3
MS39	29.9	90.7	157.6	–33.7	–66.6	156.5	29.9	90.7	337.6	33.7
MS40	29.9	90.7	188.8	–17.0	–67.3	67.7	29.9	90.7	18.8	17.0
MS41	29.9	90.7	203.8	–25.3	–62.5	32.6	29.9	90.7	23.8	25.3
MS42	29.9	90.7	160.2	–40.3	–71.0	164.1	29.9	90.7	340.2	40.3
MS43	29.9	90.7	156.4	–32.7	–65.3	156.7	29.9	90.7	336.4	32.7
MS44	29.9	90.7	162.1	–10.9	–60.3	128.9	29.9	90.7	342.1	10.9
MS45	29.9	90.7	2	17.6	69	265.2	29.9	90.7	2	17.6
MS46-49	29.9	90.7	356.3	12.7	66.3	279.9	29.9	90.7	356.3	12.7
MS50	29.9	90.7	7.9	13.5	65.8	251.3	29.9	90.7	7.9	13.5
The inclination-only mean of 56 Late Cretaceous paleomagnetic sites (groups) from the Maxiang area										**23.4± 4.1**

<u>Linzhou area</u>

The Late Cretaceous (75–68 Ma) volcanic and red beds results reported by Cao et al. (2017a).

LZ1	29.9	91.2	1.2	17.3	68.9	267.8	29.9	91.2	1.2	17.3
LZ2	29.9	91.2	168.0	-17.8	66.4	301.9	29.9	91.2	348.1	17.8
LZ3	29.9	91.2	0.9	25.5	73.5	268.0	29.9	91.2	0.9	25.5
LZ4	29.9	91.2	161.4	-37.4	71.0	337.2	29.9	91.2	341.4	37.4
LZ5	29.9	91.2	168.1	-30.9	72.9	313.2	29.9	91.2	348.1	30.9
LZ6	29.9	91.2	10.7	-0.6	58.1	250.5	29.9	91.2	10.8	-0.6
LZ7	29.9	91.2	13.7	3.0	58.8	243.9	29.9	91.2	13.7	3.1
LZ8	29.9	91.2	350.9	22.0	69.7	297.6	29.9	91.2	350.9	22.0
LZ9	29.9	91.2	6.3	34.0	77.4	242.7	29.9	91.2	6.3	34.1
LZ10	29.9	91.2	180.4	-9.4	64.8	270.2	29.9	91.2	0.4	9.3
LZ11	29.9	91.2	7.5	21.0	69.7	249.4	29.9	91.2	7.5	21.0
LZ12	29.9	91.2	191.3	-41.8	78.4	208.4	29.9	91.2	11.3	41.8
LZ13	29.9	91.2	178.5	-39.3	82.2	281.4	29.9	91.2	358.5	39.2
LZ14	29.9	91.2	6.4	14.9	66.9	254.8	29.9	91.2	6.4	14.9
LZ15	29.9	91.2	5.7	19.7	69.5	254.9	29.9	91.2	5.7	19.6
LZ16	29.9	91.2	356.4	22.8	71.7	282.4	29.9	91.2	356.4	22.9
LZ17	29.9	91.2	162.2	-3.1	57.0	305.2	29.9	91.2	342.3	3.1
LZ18	29.9	91.2	7.8	2.5	60.4	255.2	29.9	91.2	7.8	2.5
LZ19	29.9	91.2	346.0	8.7	61.2	301.2	29.9	91.2	346.0	8.6
LZ20	29.9	91.2	9.5	17.4	67.2	246.2	29.9	91.2	9.5	17.4
LZ21	29.9	91.2	17.7	30.8	69.0	216.6	29.9	91.2	17.7	30.8

The Late Cretaceous (~91–70 Ma) red beds results reported by Ma et al. (2022).

RA1	29.9	91.2	334.1	26.3	61.2	333.0	29.9	91.2	334.1	26.3
RA2	29.9	91.2	340.4	29.6	67.2	327.5	29.9	91.2	340.4	29.6
RA3	29.9	91.2	344.0	31.9	70.7	324.0	29.9	91.2	344.0	31.9
RA4	29.9	91.2	350.6	32.4	75.0	308.2	29.9	91.2	350.6	32.4
RA5	29.9	91.2	350.2	25.5	71.2	302.1	29.9	91.2	350.2	25.5
RA6	29.9	91.2	347.6	25.1	69.7	308.3	29.9	91.2	347.6	25.1
RA7	29.9	91.2	349.6	25.8	71.1	303.9	29.9	91.2	349.6	25.8
RA8	29.9	91.2	354.3	26.4	73.2	290.7	29.9	91.2	354.3	26.4
RA9	29.9	91.2	346.3	19.2	66.2	306.6	29.9	91.2	346.3	19.1
RA10	29.9	91.2	359.9	17.4	69.0	271.5	29.9	91.2	359.9	17.4
RA11	29.9	91.2	358.9	28.6	75.3	275.4	29.9	91.2	358.9	28.6
RA12	29.9	91.2	357.5	25.4	73.3	279.7	29.9	91.2	357.5	25.4
RA13	29.9	91.2	352.2	17.9	68.0	292.2	29.9	91.2	352.2	17.9

RA14	29.9	91.2	359.8	25.0	73.2	271.9	29.9	91.2	359.8	25.0
RA15	29.9	91.2	358.3	25.8	73.6	277.1	29.9	91.2	358.3	25.8
RB1	29.9	91.2	17.8	19.9	64.3	227.3	29.9	91.2	17.8	19.9
RB2	29.9	91.2	5.6	14.4	66.8	257.0	29.9	91.2	5.6	14.4
RB3	29.9	91.2	6.1	9.3	64.1	257.2	29.9	91.2	6.1	9.2
RB4	29.9	91.2	8.0	15.6	66.8	250.7	29.9	91.2	8	15.6
RB5	29.9	91.2	12.9	13.3	63.9	241.0	29.9	91.2	12.9	13.4
RB6	29.9	91.2	26.4	21.3	59.0	213.2	29.9	91.2	26.4	21.2
RB7	29.9	91.2	26.4	13.5	56.1	218.8	29.9	91.2	26.4	13.5
RB8	29.9	91.2	19.2	15.1	61.4	228.3	29.9	91.2	19.2	15.1
RB9	29.9	91.2	19.4	17.1	62.1	226.6	29.9	91.2	19.4	17.1
RB10	29.9	91.2	23.4	14.8	58.7	222.0	29.9	91.2	23.4	14.9
RB11	29.9	91.2	25.6	16.4	57.8	217.9	29.9	91.2	25.6	16.4
RB12	29.9	91.2	23.8	7.8	55.6	225.7	29.9	91.2	23.8	7.8
The Late Cretaceous (K2) Shexing Formation red beds reported by Tan et al. (2010).										
Sx1	29.9	91.2	351.6	18.8	68.3	294.1	29.9	91.2	351.6	18.8
Sx2	29.9	91.2	351.2	26.6	72.2	300.2	29.9	91.2	351.2	26.6
Sx3	29.9	91.2	355.9	24.5	72.5	284.6	29.9	91.2	355.9	24.5
Sx4	29.9	91.2	357.9	23.5	72.3	277.9	29.9	91.2	357.9	23.6
Sx5	29.9	91.2	337.1	24.1	62.6	326.9	29.9	91.2	337.1	24.0
Sx6	29.9	91.2	338.7	27.0	64.9	327.4	29.9	91.2	338.7	27.0
Sx7	29.9	91.2	343.6	23.3	66.6	315.3	29.9	91.2	343.6	23.3
Sx8	29.9	91.2	347.1	22.3	68.1	307.1	29.9	91.2	347.1	22.3
Sx9	29.9	91.2	348.4	18.4	66.8	301.5	29.9	91.2	348.4	18.3
Sx10	29.9	91.2	342.6	22.0	65.4	316.1	29.9	91.2	342.6	22.0
Sx11	29.9	91.2	344.6	14.3	63.1	306.9	29.9	91.2	344.6	14.3
Sx14	29.9	91.2	350.1	26.5	71.7	303.2	29.9	91.2	350.1	26.6
Sx15	29.9	91.2	339.4	34.1	68.2	335.0	29.9	91.2	339.4	34.1
Sx16	29.9	91.2	359.3	23.7	72.5	273.5	29.9	91.2	359.3	23.8
Sx17	29.9	91.2	357.9	25.4	73.3	278.3	29.9	91.2	357.9	25.3
Sx18	29.9	91.2	357.6	27.9	74.8	280.1	29.9	91.2	357.6	28.0
Sx19	29.9	91.2	348.7	29.8	72.6	310.4	29.9	91.2	348.7	29.8
Sx20	29.9	91.2	338.9	29.7	66.1	330.0	29.9	91.2	338.9	29.7
Sx21	29.9	91.2	343.7	37.4	72.8	333.5	29.9	91.2	343.7	37.4
Sx22	29.9	91.2	348.0	23.3	69.0	305.8	29.9	91.2	348.0	23.2
Sx23	29.9	91.2	354.2	18.1	68.7	287.1	29.9	91.2	354.2	18.1
Sx24	29.9	91.2	348.1	20.9	67.9	303.8	29.9	91.2	348.1	20.9
Sx25	29.9	91.2	337.3	15.9	59.5	320.1	29.9	91.2	337.3	15.8
Sx26	29.9	91.2	338.1	15.4	59.9	318.6	29.9	91.2	338.1	15.5
Sx27	29.9	91.2	340.3	21.5	63.8	319.7	29.9	91.2	340.3	21.5
Sx28	29.9	91.2	340.2	24.7	65.0	322.7	29.9	91.2	340.2	24.7
Sx29	29.9	91.2	347.0	17.5	65.8	304.0	29.9	91.2	347.0	17.5
Sx30	29.9	91.2	357.4	28.0	74.8	280.8	29.9	91.2	357.4	28.0
Sx31	29.9	91.2	358.5	22.4	71.7	275.9	29.9	91.2	358.5	22.4
Sx32	29.9	91.2	354.8	20.7	70.2	286.4	29.9	91.2	354.8	20.7
Sx33	29.9	91.2	350.4	28.6	72.9	304.4	29.9	91.2	350.4	28.6
Sx34	29.9	91.2	347.7	24.1	69.3	307.2	29.9	91.2	347.7	24.1
Sx37	29.9	91.2	351.3	22.2	69.9	296.8	29.9	91.2	351.3	22.2
SxB1	29.9	91.2	186.0	-19.7	69.5	254.1	29.9	91.2	6.0	19.8
SxB2	29.9	91.2	181.5	-23.5	72.3	266.4	29.9	91.2	1.5	23.5
SxB3	29.9	91.2	170.6	-22	69.6	298.5	29.9	91.2	350.6	22.1
SxB4	29.9	91.2	163.9	-20.6	65.6	312.5	29.9	91.2	343.9	20.6
SxB5	29.9	91.2	172.9	-18.8	68.7	290.8	29.9	91.2	352.9	18.8
SxB6	29.9	91.2	176.4	-23.2	71.9	282.6	29.9	91.2	356.4	23.2
SxB7	29.9	91.2	170.5	-21.6	69.3	298.5	29.9	91.2	350.5	21.6
SxB8	29.9	91.2	204.1	-28.8	63.5	209.2	29.9	91.2	24.1	28.7
SxB9	29.9	91.2	175.6	-19.8	69.9	283.9	29.9	91.2	355.6	19.8

SxB10	29.9	91.2	170.2	-21.3	69.0	299.0	29.9	91.2	350.2	21.2
The Late Cretaceous (K2) volcanic results reported by Tan et al. (2010).										
32	29.9	91.2	200.3	-47.4	72.3	180.6	29.9	91.2	20.2	47.4
31	29.9	91.2	202.5	-48.6	70.5	176.6	29.9	91.2	22.5	48.6
30	29.9	91.2	200.6	-53.3	72.1	163.1	29.9	91.2	20.6	53.3
29	29.9	91.2	186.6	-31.2	75.6	244.9	29.9	91.2	6.6	31.2
28	29.9	91.2	186.3	-28.7	74.3	248.2	29.9	91.2	6.3	28.7
27	29.9	91.2	207.2	-39.5	64.5	191.9	29.9	91.2	27.2	39.5
26	29.9	91.2	206.8	-46.5	66.5	179.7	29.9	91.2	26.8	46.5
22_25	29.9	91.2	200.5	-50.2	72.3	172.5	29.9	91.2	20.5	50.2
18_21	29.9	91.2	213.1	-48.4	61.3	173.8	29.9	91.2	33.1	48.4
13_17	29.9	91.2	216.2	-55.3	59.2	160.5	29.9	91.2	36.2	55.3
12	29.9	91.2	202.8	-32	65.7	207.2	29.9	91.2	22.8	32.0
11	29.9	91.2	197.9	-32.7	69.7	213.7	29.9	91.2	17.9	32.7
10	29.9	91.2	203.7	-42.6	68.3	189.4	29.9	91.2	23.7	42.6
9	29.9	91.2	193.6	-26.2	69.6	230.3	29.9	91.2	13.6	26.2
8	29.9	91.2	218.0	-37.3	54.7	187.0	29.9	91.2	38.0	37.3
7	29.9	91.2	203.7	-44.6	68.8	185.3	29.9	91.2	23.7	44.6
6	29.9	91.2	196.6	-45.1	75.0	189.7	29.9	91.2	16.6	45.1
5	29.9	91.2	229.1	-37	45.0	181.2	29.9	91.2	49.1	37.0
4	29.9	91.2	192.1	-38.4	76.3	215.7	29.9	91.2	12.1	38.4
3	29.9	91.2	206.3	-40.7	65.6	190.7	29.9	91.2	26.3	40.7
2	29.9	91.2	200.0	-42.8	71.6	192.3	29.9	91.2	20.0	42.8
The Late Cretaceous (K2) red beds results reported by Pozzi et al. (1982).										
1	29.9	91.2	324.0	37.0	56.3	353.3	29.9	91.2	324.1	36.6
2	29.9	91.2	333.0	43.0	65.6	355.7	29.9	91.2	333.1	42.8
4	29.9	91.2	333.0	28.0	61.0	336.0	29.9	91.2	333.0	28.0
5	29.9	91.2	328.0	47.0	62.1	5.7	29.9	91.2	328.0	47.0
7	29.9	91.2	3.0	24.0	72.4	261.5	29.9	91.2	3.0	23.9
8	29.9	91.2	338.0	29.0	65.2	330.6	29.9	91.2	338.0	29.0
12	29.9	91.2	341.0	42.0	72.2	347.2	29.9	91.2	341.0	42.0
The Late Cretaceous (K2) red beds results reported by Achache et al. (1984).										
23	29.9	91.1	-19.1	10.6	67.9	272.9	29.9	91.2	359.4	15.3
29	29.9	91.1	164.8	-40.6	58.4	315.3	29.9	91.2	338.5	11.2
30	29.9	91.1	193.1	27.0	69.3	230.8	29.9	91.2	13.6	25.6
32	29.9	91.1	-9.4	21.4	74.3	267.4	29.9	91.2	1.1	26.9
33	29.9	91.1	-20.3	29.1	65.4	321.0	29.9	91.2	341.0	24.3
34	29.9	91.1	-18.7	40.3	73.9	298.3	29.9	91.2	352.5	28.8
35	29.9	91.1	14.9	31.7	71.7	290.3	29.9	91.2	354.0	23.9
38	29.9	91.1	28.7	14.9	70.9	284.0	29.9	91.2	355.8	21.6
The inclination-only mean of 127 Late Cretaceous paleomagnetic sites (groups) from the Linzhou area										**26.3± 2.4**

<u>Naqu area</u>

The Early Cretaceous (~120.2 Ma) Duoni Formation volcanic and sedmentary results reported by Li et al. (2017).

TL01	31.3	91.9	352.7	7.2	61.5	287.3	31.4	92.0	352.8	7.4
TL04	31.3	91.9	349.9	15.2	64.6	295.8	31.4	92.0	349.9	15.3
TL05	31.3	91.9	192.1	-15.0	63.8	243.9	31.4	92.0	12.1	15.2
TL06	31.3	91.9	348.4	29.6	71.3	309.0	31.4	92.0	348.4	29.8
TL07	31.3	91.9	148.3	-20.8	54.2	333.9	31.4	92.0	328.3	20.9
TL08	31.3	91.9	349.8	13.6	63.8	295.4	31.4	92.0	349.8	13.8
TL10	31.3	91.9	340.8	13.0	59.4	311.9	31.4	92.0	340.8	13.1
TL11	31.3	91.9	330.2	9.1	51.3	324.3	31.4	92.0	330.2	9.1
TL12	31.3	91.9	14.5	10.7	60.7	241.2	31.4	92.0	14.6	10.9
TL15	31.3	91.9	20.1	9.0	57.2	232.6	31.4	92.0	20.2	9.2
TL18	31.3	91.9	17.4	22.2	64.5	229.0	31.4	92.0	17.4	22.4
TL22	31.3	91.9	6.0	9.5	62.9	258.7	31.4	92.0	6.0	9.7

TL24	31.3	91.9	356.0	12.2	64.6	281.2	31.4	92.0	356.0	12.4
TL25	31.3	91.9	1.1	20.1	69.0	268.9	31.4	92.0	1.1	20.2
TND01	31.3	91.9	348.1	17.3	65.0	300.7	31.4	92.0	348.1	17.5
TND02	31.3	91.9	1.3	27.1	73.0	267.6	31.4	92.0	1.3	27.3
TND03	31.3	91.9	358.4	19.4	68.6	276.2	31.4	92.0	358.4	19.5
TND04	31.3	91.9	359.9	16.4	67.1	272.2	31.4	92.0	359.9	16.6
TND05	31.3	91.9	354.7	15.6	66.1	285.0	31.4	92.0	354.7	15.7
The Early Cretaceous (~114–110 Ma) Zonggei Formation volcanic results reported by Li et al. (2022).										
TNZ01	31.5	92.1	5	30	74	254.5	31.4	92.0	4.9	29.9
TNZ02	31.5	92.1	4.6	29.6	73.8	256	31.4	92.0	4.6	29.4
TNZ03	31.5	92.1	9.4	31.2	73	239.7	31.4	92.0	9.4	31.0
TNZ04+05+06	31.5	92.1	5.7	33.8	76	249.1	31.4	92.0	5.7	33.6
TNZ07	31.5	92.1	11.3	27.1	70	238.4	31.4	92.0	11.3	27.0
TNZ08	31.5	92.1	27.7	16.5	55.4	218	31.4	92.0	27.7	16.2
TNZ10	31.5	92.1	355.7	28.6	73.3	286.7	31.4	92.0	355.7	28.5
TNZ11+TNZ12	31.5	92.1	352.7	30	73.2	297.1	31.4	92.0	352.7	29.8
TNZ13	31.5	92.1	2.5	13.2	65.1	266.2	31.4	92.0	2.5	13.0
The inclination-only mean of 28 Early Cretaceous paleomagnetic sites (groups) from the Naqu area										**19.6± 3.8**

Note: ID—paleopoles abbreviation used in the plot and text; Slat/Slon—latitude and longitude of the sampling location; D_s/I_s—declination and inclination in stratigraphic coordinates; Plat/Plon—latitude and longitude of the pole; Rlat/Rlong—latitude and longitude of the reference point; D_r/I_r—declination and inclination calculated for the reference points located at their studied area. The inclination-only mean is calculated following the method of Arason and Levi (2010).